

Stereocontrolled Barbier reactions for generation of homoallylic alcohols: New applications in the synthesis of natural products

Sotiris Petrides and Savvas N. Georgiades*

Department of Chemistry, University of Cyprus, 1 Panepistimiou Avenue, Aglandjia, 2109 Nicosia, Cyprus.

ABSTRACT

The Barbier reaction, a family of related transformations employing alkyl halides and carbonyl compounds in the presence of metal or metalloid to generate a new C-C bond, offers one of the most versatile methods for strategically introducing C-C connectivity in organic chemistry. The general applicability of Barbier reaction stems from the fact that it uses diverse elements from the periodic table (alkaline earth metals, transition metals, lanthanides or amphoteric elements) for *in situ* formation of a reactive nucleophilic species to attack carbonyls. Barbier conditions can be water-compatible, providing advantage over other C-C-forming reactions that employ water-sensitive organometallic species, such as organomagnesium or organolithium. Additionally, they are tolerant to various pre-existing functionalities in the substrate, thus largely circumventing the need for protection-deprotection steps in a linear synthesis. In the last decade, a resurgence in the application of Barbier reactions has occurred, especially in the context of natural product synthesis, where this transformation is quickly proving to be a powerful tool. Since multiple (bioactive) natural product families feature homoallylic alcohol motifs as part of their structures, Barbier reactions involving allyl halides and carbonyl compounds as precursors to generate such homoallylic alcohols are becoming a method of choice. This review focuses on selected

cases where homoallylic alcohols are the resulting products and where the Barbier reaction is stereocontrolled, with emphasis on the stereocontrolling elements in synthesis design and the models employed to rationalize the observed stereochemical outcome.

KEYWORDS: Barbier reaction, stereocontrol, homoallylic alcohol, natural products.

CONTENTS

1. Introduction
2. Barbier allylation protocols: An overview
3. Regio- and stereoselectivity considerations in Barbier reactions
4. Case studies of stereocontrolled Barbier reactions in the synthesis of natural products
 - 4.1. Added chiral ligand-controlled stereoselectivity
 - 4.1.1. (+)-Costunolide, Mukulone and analogues
 - 4.2. Substrate chirality-controlled stereoselectivity
 - 4.2.1. Deoxyelephantopin
 - 4.2.2. Phorbin A
 - 4.2.3. (+)-Chatansin
 - 4.2.4. Axinellamines A & B
 - 4.2.5. Cyanolide A
 - 4.2.6. (+)-Mikanokryptin
 - 4.2.7. Slovanolide, Montanolide, Nortrilobolide
 - 4.2.8. Sinodiellide A
 - 4.2.9. (-)-8-Epigrosheimin

*Email id: georgiades.savvas@ucy.ac.cy

- 4.2.10. Natural product analogues 4-Epi-Fagomine, 3,4-Dihydroxypipelic acid, Dihydroxyindolizidine
- 4.2.11. Cochliomycin C, Paecilomycin F, (3*R*,4*S*)-4-Hydroxylasiodiplodin, Verbalactone, Stagonolide C, (-)-Cleistenolide, (+)- β -Conhydrine
- 4.2.12. (+)-Swainsonine
- 4.2.13. Uprolide D analogue
- 4.2.14. (-)-Ansellones A and B, (+)-Phorbadiolone

5. Conclusions and outlook

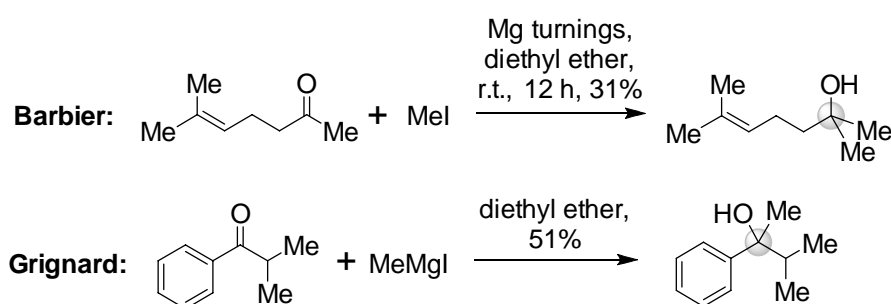
1. Introduction

Since the nascent stages of the field of Organic Chemistry, the ability to connect carbon segments for the purpose of chain elongation, branching and functionalization has been extremely desirable. Carbon-carbon bond formation remains a vital part of modern synthetic chemistry, with synthesis being heavily dependent on transformations of this type.

It is noteworthy that until the end of the 19th century, zinc was the most prominent metal used in C-C coupling reactions. P. Barbier and V. Grignard were the first to utilize magnesium in carbonyl addition reactions (Scheme 1), paving the way towards the application of many other metals in C-C bond forming reactions, in the years that followed. An early example by Barbier involved the use of magnesium turnings in diethyl ether solution of 6-methylhept-5-en-2-one, with slow addition of methyl iodide, for the production of 2,6-dimethylhept-5-en-2-ol [1]. Modest yields and poor reproducibility discouraged Barbier from further exploring the

scope of this reaction. However, Grignard, a former student of Barbier's, investigated similar conditions, but instead of generating and consuming the *in situ* produced nucleophilic species in one pot, he isolated the organomagnesium intermediate, then used it in a second step for carbonyl addition, achieving better yields and excellent reproducibility. The Grignard reaction led to a 1900 publication, after which it soon became quintessential to organic chemists (and still remains today), since it provided a clear path towards primary, secondary and tertiary alcohols from simple carbonyl precursors and alkyl or aryl halides, in a high yielding and reproducible manner. Grignard was awarded the Chemistry Nobel prize in 1912 for this discovery (shared) [2].

Both the Barbier and Grignard are classified as nucleophilic additions to carbonyl compounds and both utilize alkyl halides and carbonyl compounds as substrates in the presence of the metal or metal salt, generating the organometallic species *in situ*, with the final product being an alcohol of higher substitution compared to the carbonyl starting material. Their main difference lies in the way the organometallic species is generated prior to attack on the electrophilic carbonyl moiety. In the Grignard reaction, the alkyl halide initially reacts with the Mg, generating the organometallic species, which is then added to the carbonyl compound in a separate step and in a controlled fashion. Instead, the Barbier reaction is a one-pot procedure with the alkyl halide, metal and carbonyl compound introduced into the reaction vessel simultaneously, allowing the *in-situ* produced organometallic species to react directly with the carbonyl.



Scheme 1. Early examples of tertiary alcohol generation from ketones, reported independently by Barbier [1] and Grignard [2].

Historically, the Grignard reaction is more widespread. However, more recent variants that maintain the one-pot nature of the original Barbier reaction are today described as Barbier-type reactions. These exhibit more desirable characteristics since they manage to by-pass a major limitation of the Grignard reaction, namely its requirement for strictly anhydrous conditions during formation, isolation and handling of the reactive organomagnesium intermediate, due to its quenching upon contact with water/moisture. This is achieved by replacing the magnesium with other metals or amphoteric elements that are tolerant to moisture or even get activated by the presence of water. Hence, under the general title of Barbier reaction – to discriminate from Grignard reactions –, a huge range of reaction conditions have been investigated, and combinations of zero-valent metals and metal salts, as well as bimetallic systems that are tolerant to moisture have been determined. Vast literature now exists, dedicated to this reaction and to its optimization. Several protocols even introduce water as solvent, which can minimize or completely eliminate the expensive and possibly toxic organic solvents from these protocols, while the use of benign metal salts can remove the rare, expensive and/or toxic zero-valent metals used in some protocols. This constitutes progress towards introducing this

category of reactions to the realm of “green chemistry”. In parallel to condition optimization, the scope of the Barbier reaction has also expanded beyond alkylation of simple aldehydes and ketones, to include a wide variety of both carbonyl and organohalide substrate types. Alkyl, allyl, vinyl, benzyl and propargyl halides were used in a vast array of protocols, in conjunction to substrates such as aldehydes, ketones, esters, imines, imides, nitriles, azo compounds and many more, to produce a variety of products with extended carbon frame [3-7].

A special place among the carbon skeletons that can be accessed via Barbier coupling hold those comprising a homoallylic alcohol. Homoallylic alcohols can be constructed from carbonyl compounds and allyl halides, by applying Barbier allylation protocols. Homoallylic alcohols are very versatile synthons often required in a variety of synthetic procedures towards biologically relevant natural products, since many natural product families contain this motif as part of a linear chain or ring system (Figure 1). The latent functionality of the produced homoallylic alcohol is very useful in synthetic planning, as it can undergo a plethora of diversity-generating reactions (e.g., oxidation/reduction, cycloaddition, epoxidation, hydration, hydrogenation, dihydroxylation, olefin

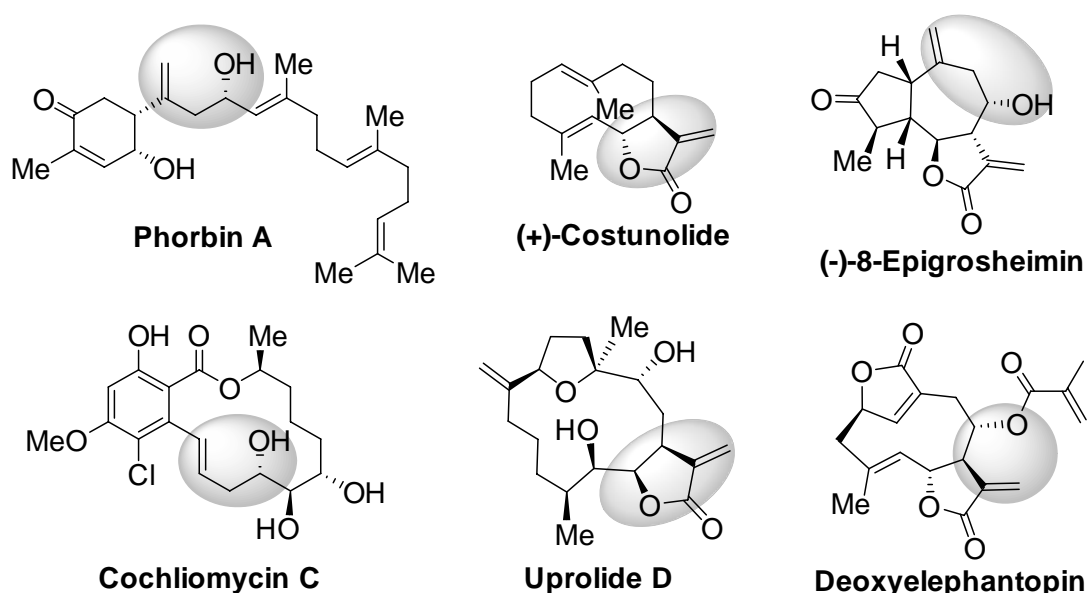


Figure 1. Representative examples of natural product structures containing the homoallylic alcohol motif (highlighted in grey ovals), which can be constructed *via* Barbier allylation of carbonyl precursors.

metathesis, etc.), thus paving the way for downstream transformations. Importantly, application of stereo- and enantioselective allylation protocols may lead to the production of one or two stereocenters in a single synthetic step. Construction of carbon chains bearing a sequence of stereocenters is also possible through this type of reaction. As Barbier allylations have dominated the field of natural product synthesis in recent years, forging new frontiers in stereocontrol and construction of complex molecular architectures, they will be the focus of this review article.

2. Barbier allylation protocols: An overview

A significant portion of the periodic table elements has been utilized in Barbier allylation reactions. After the initial use of Mg, an alkaline earth metal, also transition metals, metalloids as well as lanthanoids were introduced into Barbier reaction protocols (Figure 2), each with a different degree of success.

Many reaction protocols include some form of activation for the metal mediators used. In the case of metals that can form a layer of metal oxide on their surface, due to the presence of moisture, or metals that exhibit inherently low reactivity, activation of the metal surface can significantly

enhance the overall reaction yield. This activation can occur in the form of mild heating, sonication or inclusion of a reactive additive in the reaction mixture. Synthetic protocols of Barbier allylation that involve surface activation are abundant in the literature and typically concern readily corroded or generally unreactive metal mediators, such as manganese, zinc, aluminum, gallium and lead.

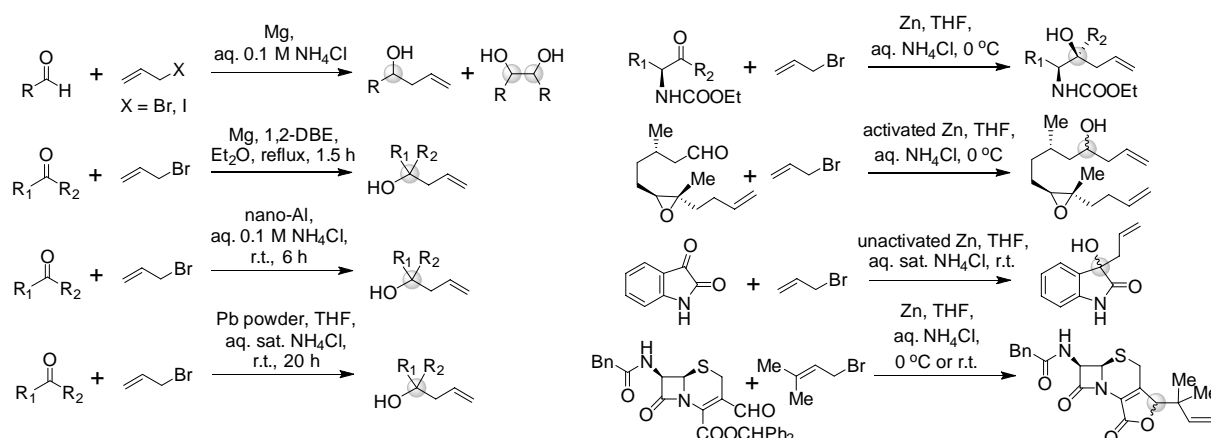
The use of additives such as 1,2-dibromoethane (DBE) or NH_4Cl in the reaction medium can ensure the removal of the retardive metal oxide layer, exposing the reactive zero-valent metal underneath [8, 9]. Scheme 2 depicts some of the protocols that utilize such forms of activation for the metal mediator used [10-20].

Mild heating of the reaction mixture is another way of causing surface activation of the metallic mediator. This was implemented in a series of Barbier reactions by Wang *et al.* using Ga metal, in the absence of any additives [21]. Interestingly, the reaction exhibited solvent dependence, favoring a *syn* diol product in water but *anti* diol product in THF (Scheme 3).

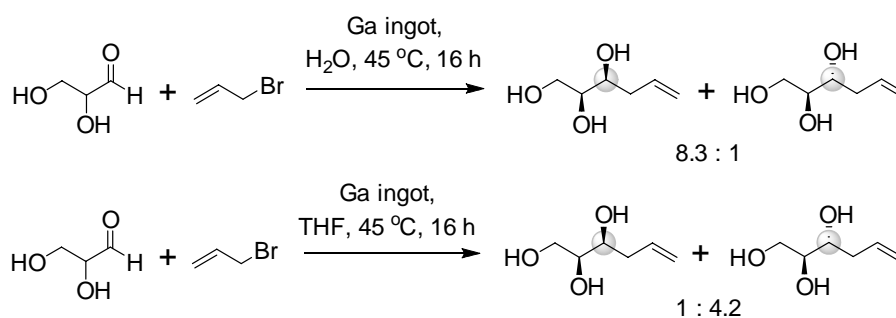
Sonochemistry was also used instead of chemical additive in order to enhance reactivity of the metal mediator (Scheme 4) [22-25]. Ultrasonic exposure can rid the metal surface of any retarding

H																He	
Li	Be										B	C	N	O	F	Ne	
Na	Mg										Al	Si	P	S	Cl	Ar	
K	Ca	Sc	Ti	V	Cr	Mn	Fe	Co	Ni	Cu	Zn	Ga	Ge	As	Se	Br	Kr
Rb	Sr	Y	Zr	Nb	Mo	Tc	Ru	Rh	Pd	Ag	Cd	In	Sn	Sb	Te	I	Xe
Cs	Ba	La	Hf	Ta	W	Re	Os	Ir	Pt	Au	Hg	Tl	Pb	Bi	Po	At	Rn
Fr	Ra	Ac	Rf	Db	Sg	Bh	Hs	Mt	Ds	Rg	Cn	Nh	Fl	Mc	Lv	Ts	Og
			Ce	Pr	Nd	Pm	Sm	Eu	Gd	Tb	Dy	Ho	Er	Tm	Yb	Lu	
			Th	Pa	U	Np	Pu	Am	Cm	Bk	Cf	Es	Fm	Md	No	Lr	

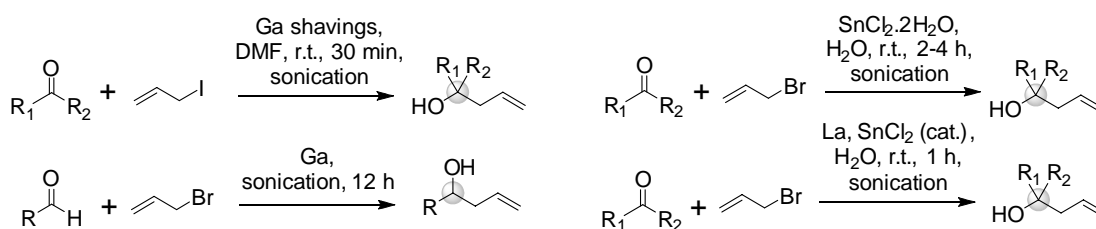
Figure 2. Periodic table, with metal-mediators and metal catalysts employed in Barbier-type coupling protocols highlighted in black square frames.



Scheme 2. Representative chemically-activated metal-catalyzed Barbier allylation conditions [10, 12-18].



Scheme 3. Activation of Ga metal in Barbier reactions by mild heating [21].



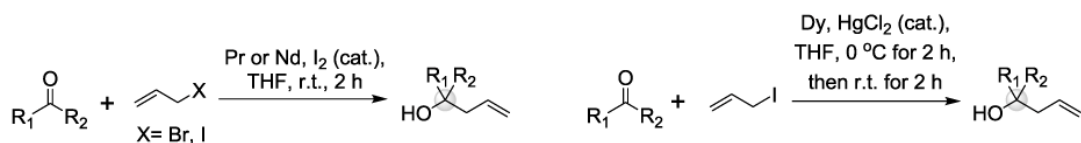
Scheme 4. Barbier allylation protocols employing activation of the metal mediator by sonication [22-25].

contaminants, while at the same time promotes the overall reaction through cavitation phenomena [26, 27].

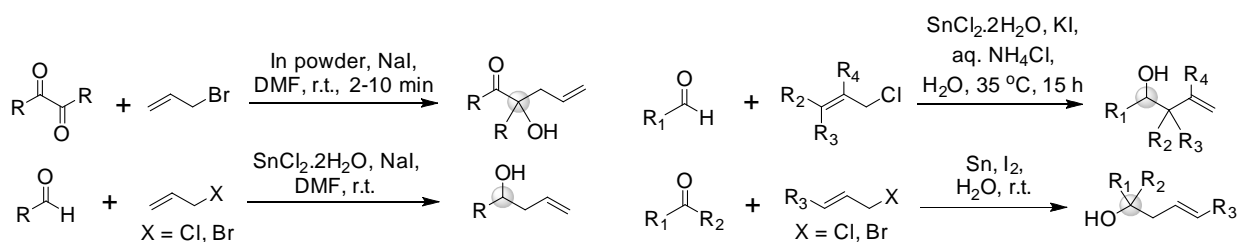
Co-catalysis of the Barbier reaction was also reported in some cases, most notably when lanthanides lanthanum [25] (Scheme 4, last entry), praseodymium [28], neodymium [29] and dysprosium [30] (Scheme 5) were used as the metal mediators. In these cases, an initiator (I_2 , $SnCl_2$ or $HgCl_2$) was

necessary in catalytic amounts in order to promote the allylation reaction.

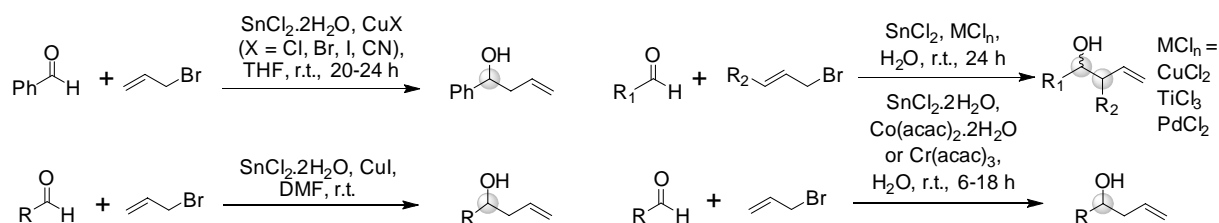
Other additives were also reported to enhance conversion in Barbier allylations (Scheme 6), such as NaI in indium- [31] and tin-mediated [32] protocols and KI in $SnCl_2$ -mediated protocols [33] (through Finkelstein reaction, producing a reactive allyl iodide from a less reactive allyl chloride), while *in situ* generation of SnI_2 , from



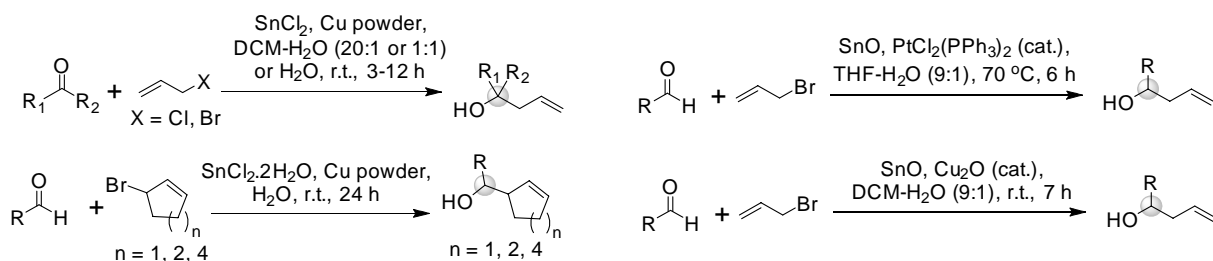
Scheme 5. Use of initiator in lanthanide-mediated Barbier allylation reactions [28-30].



Scheme 6. Barbier allylation protocols employing iodide salts for Finkelstein activation of unreactive allyl halide components [31-34].



Scheme 7. Barbier allylation protocols employing transition metal salts as co-catalysts to activate both reaction components [35-41].



Scheme 8. Barbier allylation protocols employing heterogeneous Cu(0) or β -SnO co-catalysts [42-45].

Sn and I₂ did not require any additional iodide salt [34].

Alternatively, some protocols have exploited transition metal salts as co-catalysts in SnCl₂-mediated cases (Scheme 7), such as Cu(I) [35, 36], Cu(II) [37-39], Ti(III) [39, 40], Pd(II) [39], Co(II) [41] and Cr(III) [41]. Their ability to

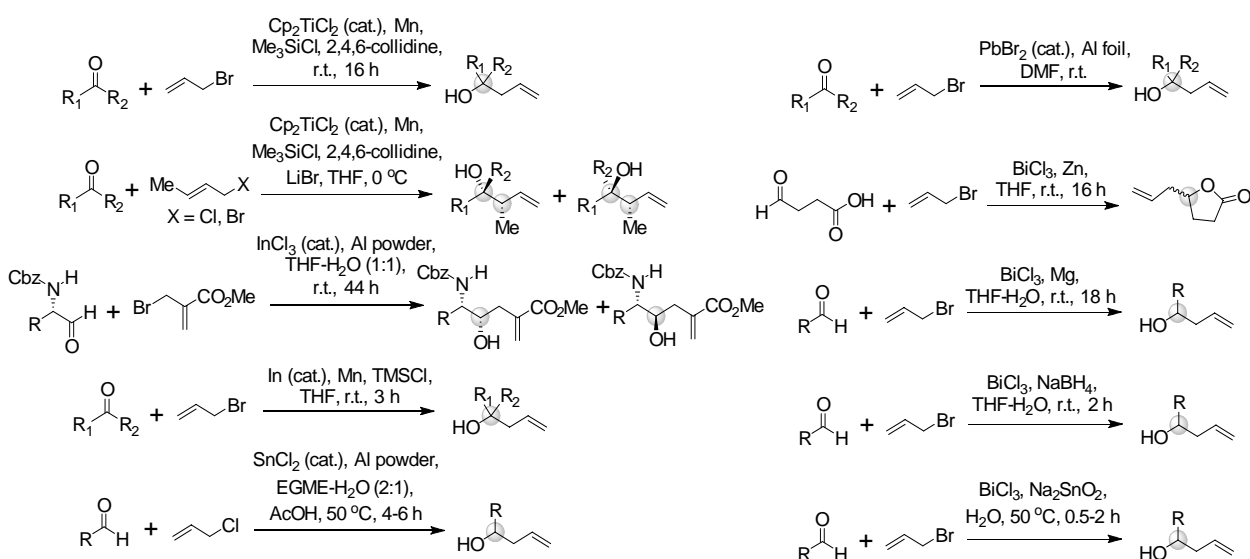
combine allyl halide component activation, as π -complex, with carbonyl component activation, as σ -complex, has been suggested [37]. Redox events may take place during these reactions.

Heterogeneous catalysis has also been employed, with Cu(0) in SnCl₂-mediated cases [42, 43] and β -SnO in Pt(II)- [44] or Cu₂O-catalyzed cases [45]

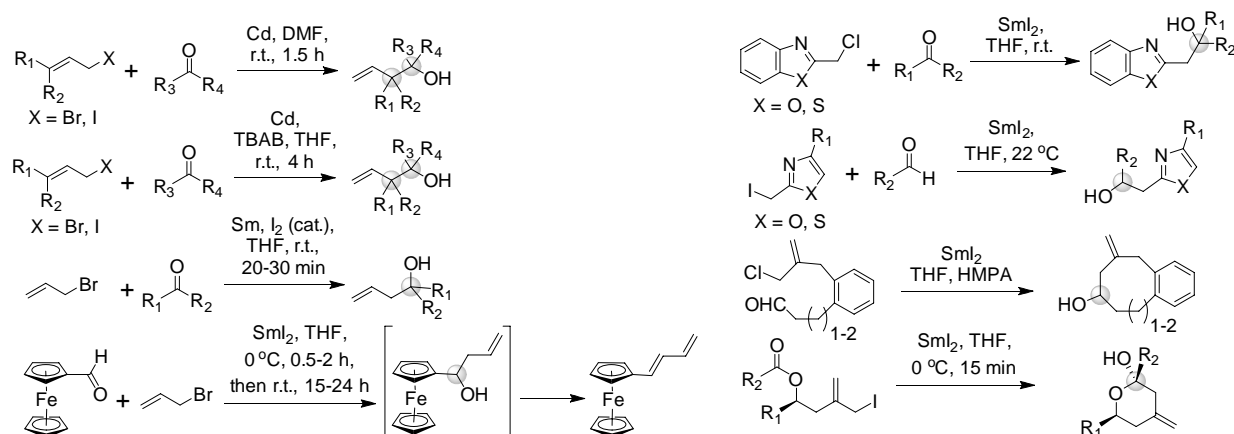
facilitating the reaction by providing the solid surfaces for reactant association (Scheme 8). Some of these protocols are compatible with biphasic solvent systems, which provide flexibility as to the type of substrates.

Through the course of the Barbier reaction, the metal mediator undergoes redox. To develop catalytic variants of the reaction, where a precious metal mediator can be recycled through several catalytic cycles, additional redox reagents are required. If a zero-valent metal is used, it is initially oxidized in the oxidative addition step (reducing the allylic carbon) and then must be reduced back to its original oxidation state. Taking this into consideration, a multitude of protocols were reported, introducing a reducing agent in the reaction mix, able to regenerate the active metal species *in-situ*. This catalytic approach minimizes the amounts of expensive and possibly toxic metals required. Alternatively, if the catalytic species needs to be generated from a metal salt, the reaction requires an initial reduction step prior to the start of the catalytic cycle. Several catalytic protocols currently exist, many of which involve bimetallic systems (Scheme 9), such as titanocene-Mn [46, 47], In-Al [48], In-Mn [49, 50], Sn-Al [51, 52], Pb-Al [53] and Bi with a variety of zero-valent metals [54-57] or other reducing agents [58, 59].

As it is evident from the schemes above, many variants of Barbier reaction can be conducted in aqueous media, especially when the protocol involves water-soluble salts. Additionally, in instances of reactions mediated by indium, tin and bismuth, water may often be used as the sole reaction solvent, in the context of “green chemistry” [60-66]. This can be attributed to their resistance to corrosion and ability to withstand the presence of air and moisture without any loss of reactivity. Although most of the metals discussed in the present review can mediate the Barbier allylation in aqueous media, another group of metals, such as cadmium [67, 68], praseodymium [28], neodymium [29], samarium [69-83] and dysprosium [30], require strictly anhydrous conditions. This is most likely a consequence of their very low reduction potential, which renders them able to reduce water, releasing hydrogen gas. Pr, Nd and Dy have been discussed above (Scheme 5). Various conditions for Cd have been reported, including ones utilizing phase-transfer catalysts [68], while SmI_2 (pre-formed or *in situ* generated) has proved to be one of the most versatile mediators of Barbier reaction, often preferred in the synthesis of medicinally relevant organic scaffold classes and natural products [73-83], due to its compatibility with diverse functionalities (Scheme 10).



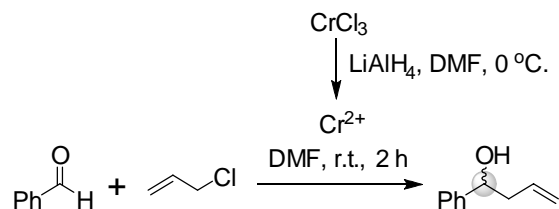
Scheme 9. Examples of bimetallic redox Barbier allylation protocols [46-49, 51, 53, 56-59].



Scheme 10. Examples of Barbier allylation protocols involving Cd and SmI₂ that require strictly anhydrous conditions [67, 68, 71-74, 77, 80].

It is worth mentioning a variant of the Barbier reaction between aldehydes and allyl halides catalyzed by CrCl₂/NiCl₂, known today as the Nozaki-Hiyama-Kishi (NHK) reaction. H. Nozaki and T. Hiyama first reported the coupling of benzaldehyde and allyl chloride (1977) utilizing a Cr(II) salt generated from reduction of chromic chloride with LiAlH₄ (Scheme 11) [84]. In 1986, in the course of synthesizing Palytoxin, Y. Kishi and his co-workers reported that NiCl₂ impurities could co-catalyze the reaction and were essential for its success and reproducibility [85]. The research group which reported the original reaction also reported the same findings around the same time [86]. NHK reaction has rather narrow focus, being applicable solely to aldehydes and excluding other precursor groups such as ketones, esters, amides, nitriles etc. It has been reviewed by others [87], most notably its asymmetric applications in natural product synthesis [88-91], and will not be discussed extensively herein.

Finally, organoboron and organosilicon cases that closely resemble Barbier reactions are not strictly classified as such, since they typically involve pre-formed reagents, in contrast to the *in-situ* generated organometallic reagents that are the defining feature of the Barbier. While a multitude of examples have been reported in organic synthesis over the years involving allylboron and allylsilicon reagents, and both these categories have become essential in the context of complex



Scheme 11. First reported C-C coupling reaction catalyzed by *in situ* generated Cr(II) [84].

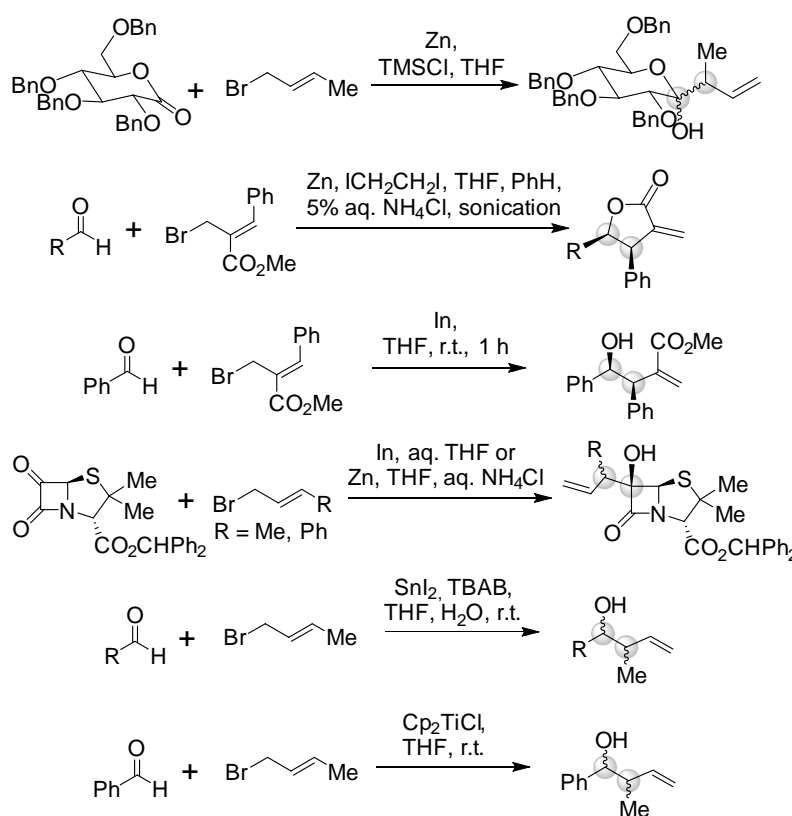
(stereocontrolled) molecule synthesis, they have been reviewed exhaustively by others [92-95] and are not included in this review.

3. Regio- and stereoselectivity considerations in Barbier reactions

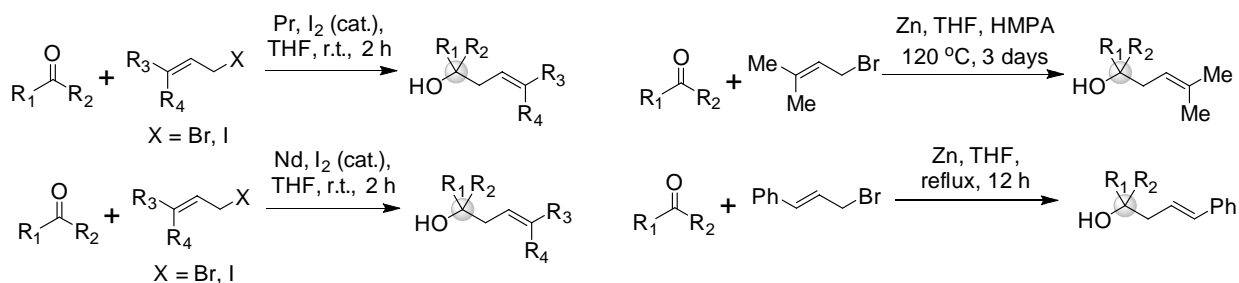
Barbier reactions can be exploited from a regioselectivity perspective, depending on the actual conditions used. Specifically, when γ -substituted allyl compounds are employed as one of the coupling components in a Barbier allylation reaction, two distinct possibilities exist: Either the α -adduct can be produced or the γ -adduct, with the latter revealing a rearrangement of the allylic system to react with the carbonyl component *via* the distal carbon. Although regioselectivity heavily depends on the bulkiness of the γ -substituent(s) as well as the solvent system and the presence of additives in the reaction mixture, the metal mediator species is known to influence the outcome to a

great extent. While some of the metals able to catalyze the Barbier reaction do not exhibit any apparent regioselectivity, some others notably lead to one of the two possible regioisomers. Among these, zinc [17, 18, 96-99], tin [33, 34, 64-66, 100, 101], titanium [47, 102] and indium [63, 98, 99] have been shown to exhibit significant regioselectivity, producing the γ -adduct(s) as the major, if not exclusive, product(s) (Scheme 12).

Contrary to most regioselective Barbier protocols that yield predominantly the γ -adduct, Barbier reactions mediated by praseodymium [28] and neodymium [29], that utilize γ -substituted allyl halides, produce almost exclusively the α -adducts (Scheme 13). This could be very helpful in synthesis, since other α -selective protocols in the literature require either long reaction times at high temperature or very polar solvents (Scheme 13) [20, 103].



Scheme 12. Examples of γ -regioselectivity in Barbier reaction protocols [96-100, 102].



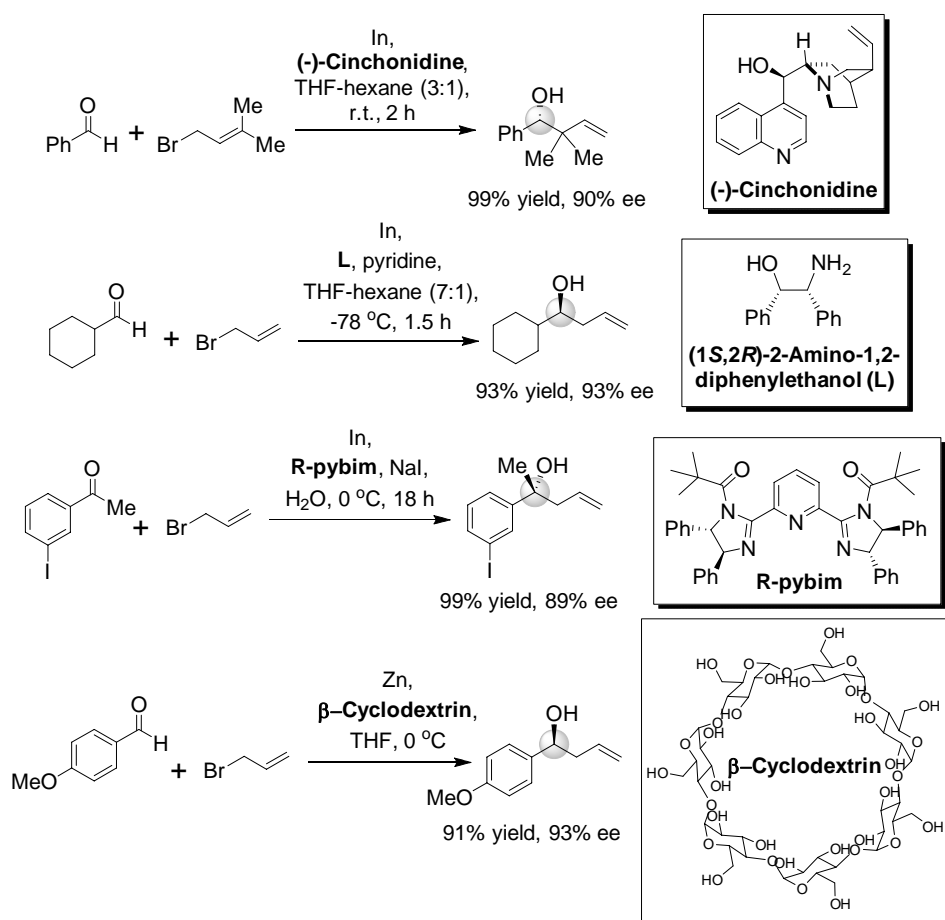
Scheme 13. Examples of α -regioselectivity in Barbier reaction protocols: lanthanide-based, room-temperature, short-time protocols (left) [28, 29] vs. zinc-based, high-temperature, long-time ones (right) [20, 103].

Stereoselectivity is another major consideration of Barbier protocols, since this reaction can create chiral centers. The simplest scenario is the generation of one chiral center from allylation of a pro-chiral carbonyl compound. Various protocols have been developed that employ diverse chiral ligands or additives (Scheme 14).

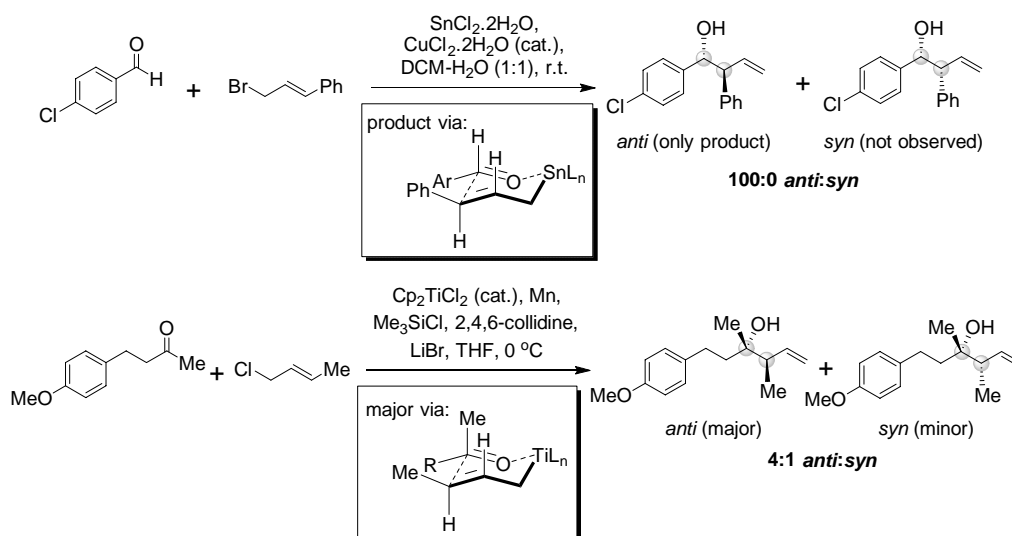
For example, alkaloid (-)-Cinchonidine has been shown to control absolute stereochemistry, leading to high enantioselectivity in some of the studied cases, in In-promoted allylation of aldehydes in THF-hexane [104]. Another In-mediated protocol employed (1*S*,2*R*)-2-amino-1,2-diphenylethanol at low temperature [105]. More recently, R-pybm, a chiral pyridyl-bis(imidazoline), was successfully employed in In-promoted allylation of ketones in water [106]. Sugar-based chiral additives have

also been exploited, with β -Cyclodextrin exhibiting promise in achieving high enantioselectivity in a Zn-mediated case [107].

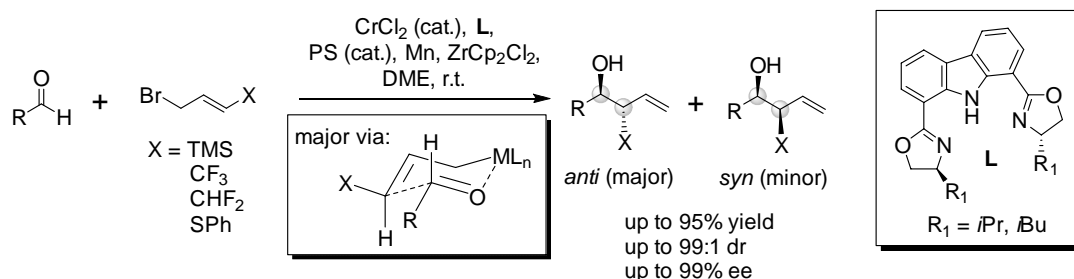
Barbier reactions that proceed in a γ -regioselective fashion may generate 2 adjacent chiral carbon centers simultaneously. In these cases, the relative stereochemistry (*syn* vs. *anti*) must be defined. Relative stereochemistry is dictated by the indigenous ability of the metal to organize a cyclic transition state. For example, tin [37, 39] and titanium [47], both strong Lewis acids that favour a cyclic transition state for the addition, have been found to exhibit high *anti* diastereoselectivity when starting from *trans* halides. In such cases, a 6-membered Zimmermann-Traxler-like transition state can be invoked to explain the relative stereochemical outcome (Scheme 15). This positions the largest



Scheme 14. Examples of highly enantioselective, metal-mediated Barbier allylations of aldehydes and ketones, using various chiral ligands or additives [104-107].



Scheme 15. Cases of Barbier reaction using a strongly Lewis acidic metal mediator, that enables the assembly of a closed, 6-membered Zimmerman-Traxler-like transition state [37, 47]. This cyclic organization leads to control of relative stereochemistry, which favours *anti* over *syn* product, in case of *trans* allyl halides. For *cis* allyl halides, *syn* product would be expected to be major, albeit with lower diastereoselectivity.



Scheme 16. Example of Barbier/NHK variation that employs coordinating metal and a chiral ligand to control both relative and absolute stereochemistry of the 2 newly-formed chiral centers [108].

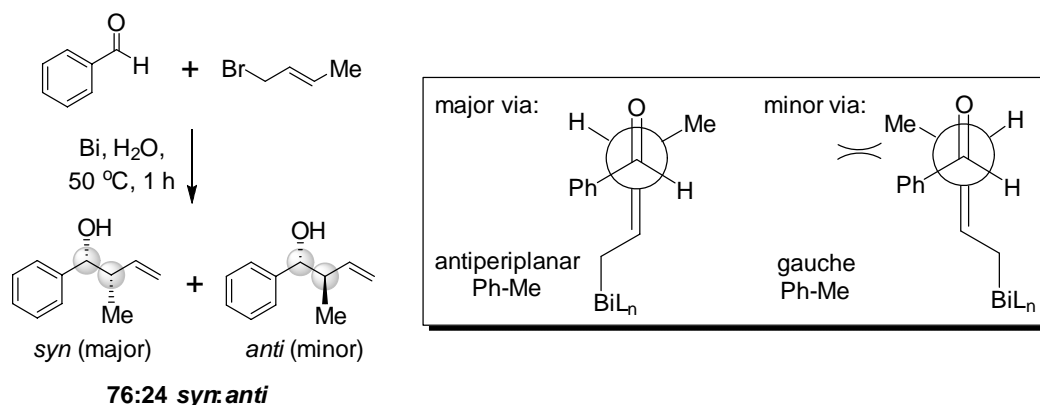
substituents of both the allyl halide and carbonyl compound pseudo-equatorial, to minimize 1,3-diaxial interactions. Following a similar arrangement, *cis* allyl halides would be expected to demonstrate lower diastereoselectivity, as they would inevitably place the large substituent pseudo-axial.

In Barbier reaction systems that generate 2 chiral carbon centers, it is also possible to control both relative and absolute stereochemistry by combining the organizing ability of the metal that enables transfer of stereochemical information, with a bias introduced by a chiral ligand (Scheme 16) [108].

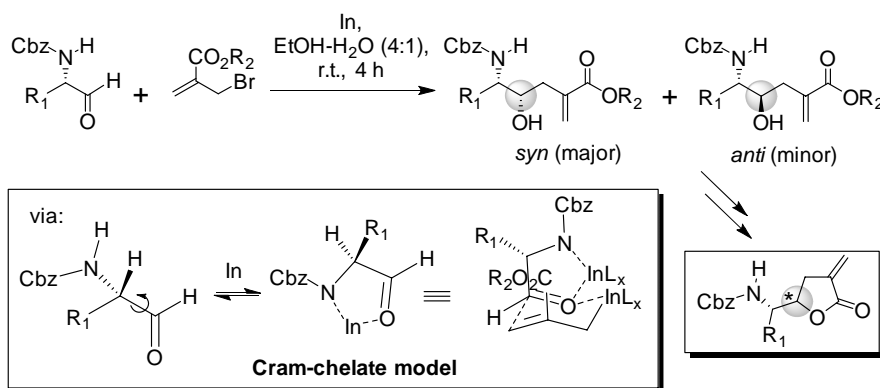
A less investigated case is that of large and soft metals, such as bismuth, which appear to favour

open/acyclic transition states, leading preferentially to the formation of *syn* products, regardless of the geometrical isomer of allyl halide used (Scheme 17) [54, 58, 59]. An acyclic transition state can be invoked to rationalize the major product, with the large substituent at the distal position of the double bond being placed antiperiplanar to the large group of the carbonyl compound, thus minimizing sterics.

Another interesting scenario that often occurs in the context of natural product synthesis is the existence of chirality at a position α - to the carbonyl, which in its own right may affect the stereochemical outcome by exerting an influence in the transition



Scheme 17. Case of Barbier reaction catalyzed by bismuth, leading to *syn* as the major product from a *trans* allyl bromide, *via* antiperiplanar open/acyclic transition state [59].

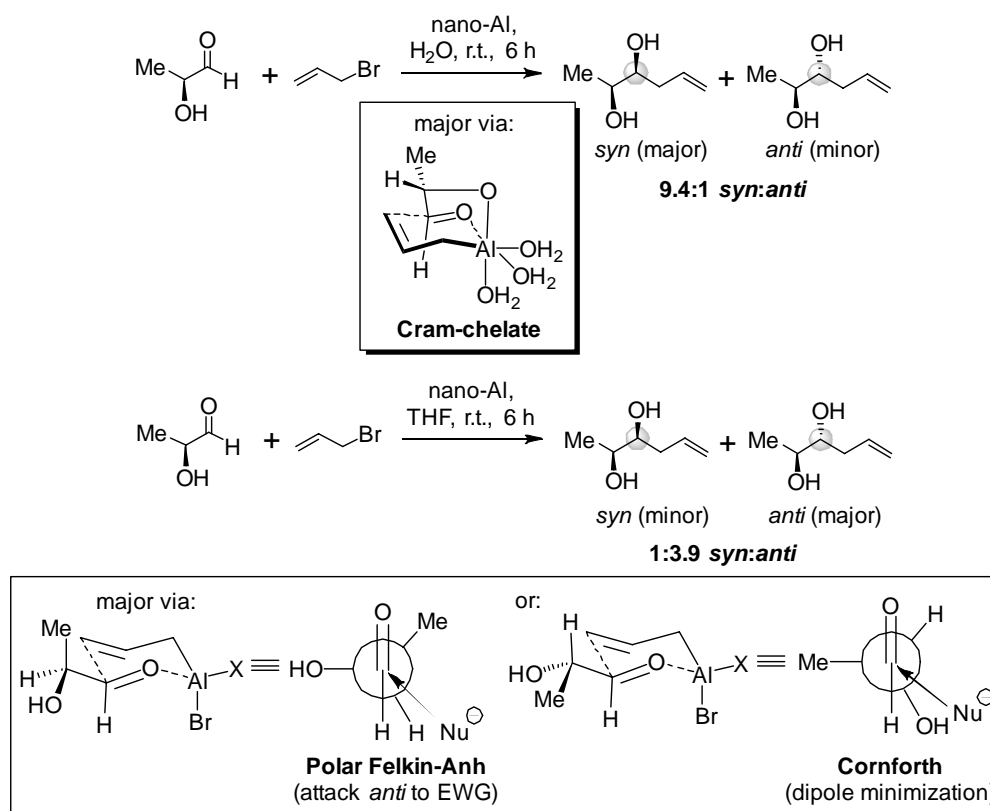


Scheme 18. In-mediated Barbier allylation as a key step towards α -methylene butyrolactones, where stereoselectivity is controlled by a Cram-chelate complex [109].

state. Especially if a substituent on an α -chiral carbon has Lewis-basic character, it can coordinate onto the metal mediating the Barbier reaction (Lewis acid), in addition to the coordination of the carbonyl, thus creating a bidentate chelation complex. This forces the α -chelating substituent and the carbonyl to be oriented nearly co-planar (eclipsed), guiding attack of the nucleophile to the less sterically hindered face of the chelation complex. This scenario is often referred to as the Cram-chelate model. Some of the examples that follow will showcase this scenario, and how chelation controls the stereoselectivity of the Barbier allylation.

A Barbier allylation protocol utilising indium in an ethanol/water solvent system was demonstrated

by Steurer *et al.* in their studies for synthesis of α -methylene butyrolactones, which heavily depended on the Cram-chelate model for achieving stereoselectivity (Scheme 18) [109]. The protected amino group on the α -chiral center can eclipse the carbonyl with a simple rotation. Loss of the acidic proton in the presence of indium cations can generate a chelate complex with indium acting as the Lewis acid. The allyl-indium reagent can then approach from the face of the chelate that poses the lowest steric hindrance associated to the R_1 substituent. This becomes apparent from the results obtained by this group, observing that increasing the size of the R_1 group increased diastereoselectivity in favor of the *syn* product, reaching up to 97:3 dr when R_1 was *tert*-butyl.



Scheme 19. Solvent effect on the stereoselectivity of an Al-mediated Barbier allylation reaction [13].

A similar case is showcased below with aluminum as Barbier promoter (Scheme 19) [13]. In water, the α -OH can ionize and coordinate on the Al center, forming a chelate, with the back side more hindered, enabling placement of the allyl nucleophile at the front and leading to the *syn* product as the major product. The transition state is described by the Cram-chelate model. However, the nature of the solvent can have a very strong influence on the stereochemical outcome in these reactions. In THF, for example, the neutral α -OH does not allow chelation, and the stereochemical outcome (*anti* product is major) can be rationalized only by invoking the polar Felkin-Anh model or a modified Cornforth model. A similar case of stereochemistry switch upon solvent change is observed in the Ga example of Scheme 3 [21]. Stereoselectivity can be guided towards the alternative diastereomer also by introducing bulky substituents in appropriate positions of the substrates or additives in the reaction media that will alter either the ability of functional groups to coordinate or their steric bulk.

4. Case studies of stereocontrolled Barbier reactions in the synthesis of natural products

Homoallylic alcohols, the product of Barbier reaction between allyl halides and carbonyl compounds are an important synthon in organic chemistry as well as a characteristic motif in many natural product families, including bioactives. The unique configuration of stereocenters in bioactive natural products affords a unique structure and 3D shape which enables each of them to interact with its biological target, in a way that induces a specific response. Thus, it is imperative that those stereocenters be preserved along with the overall spatial arrangement during synthesis, in order to recreate the desired biological activity and avoid serious side effects upon pharmaceutical application.

In this section, representative examples of stereocontrolled Barbier reactions for the strategic allylation of carbonyl precursors, selected from recent natural product syntheses will be examined, highlighting the stereocontrolling elements and

showcasing the various models used to explain how regio- and diastereoselectivity is achieved.

4.1. Added chiral ligand-controlled stereoselectivity

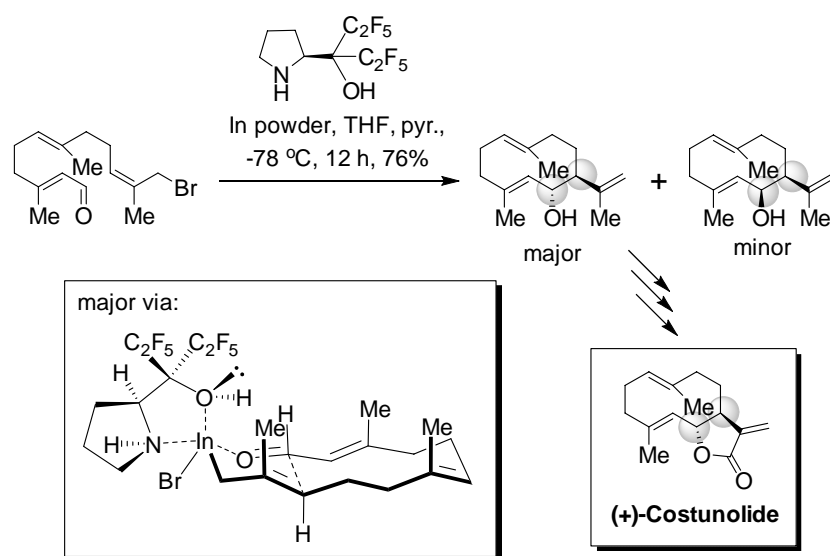
In cases where the precursors contain no stereocenters able to direct the stereochemical outcome of the Barbier reaction, the result is generation of a mixture of enantiomers or diastereomers. Such mixtures often require specialized chiral separations to resolve into their individual, enantiomerically pure components, while they also lower the yield of the desired stereoisomer. In such scenarios, an external chiral ligand can be added to the system, in order to direct the reaction stereoselectivity towards the desired product.

4.1.1. (+)-Costunolide, Mukulone and analogues

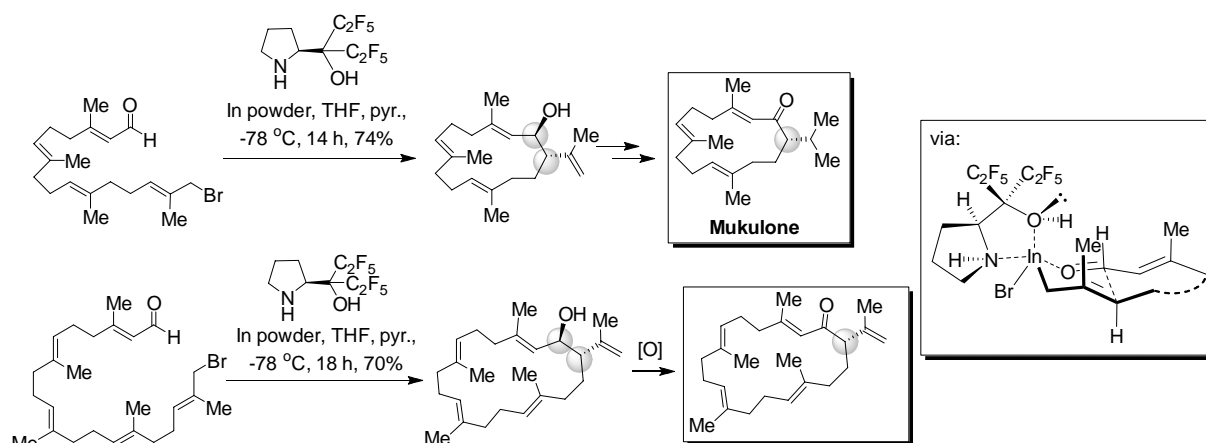
Such a case was encountered by Corey and co-workers in their synthetic studies towards various targets from cyclic sesquiterpenoid families [110]. Since the polyprenyl hydrocarbon chain they selected as starting material, comprising both allyl halide and aldehyde moieties at its two termini, lacked any chiral centers that could influence the stereoselectivity, a chiral ligand had to be introduced. It was found that between 1,1-diphenyl prolinol and 1,1-bis-pentafluoroethyl prolinol, the

latter could enhance the stereoselectivity to a greater extent. The use of this chiral ligand in an indium-mediated Barbier allylation reaction at low temperature allowed for very high, up to complete, stereoselectivity in cyclization reactions leading to 10-, 14- and 18-membered macrocycles. A 10-membered example is shown in Scheme 20.

The 1,1-bis-pentafluoroethyl prolinol can coordinate on the indium through the N and O atoms, with the proline ring imposing a steric barrier to the aldehyde on one face of the allyl-metal species. This forces the carbonyl terminus of the polyprenyl chain to approach from the opposite face, thus rendering the coupling reaction stereoselective. A chair-like transition state may represent the lowest-energy conformer, due to minimization of torsional/transannular strain. The occurrence of a minor diastereomer in the reaction mix may be indicative of an alternative orientation of the carbonyl, corresponding to a higher-energy transition state. It is proposed that the chiral ligand coordinates on the metal in a way that gives rise to a highly stable coordination complex, limiting alternative orientations of the carbonyl - albeit the hydrogen-bonding ability of the OH may provide window for one - thus elevating the diastereoselectivity of major to minor product to 14:1.



Scheme 20. Intramolecular In-mediated Barbier allylation employing a prolinol-type chiral ligand was a key step in the stereoselective synthesis of (+)-Costunolide [110].



Scheme 21. Intramolecular In-mediated Barbier allylation protocol involving a prolinol chiral ligand applied in the syntheses of Mukulone and 18-membered counterpart [110].

In the examples shown in Scheme 21, the same approach was applied for the generation of larger macrocyclic terpenoid systems [110]. In these cases, only one diastereomer could be observed, likely due to the reduction of transannular strain in the transition states of these systems relative to the smaller 10-membered system, a difference that favors stabilization of the lowest-energy complex. Although for these 14- and 18-membered macrocycles longer reaction times were needed (14 h and 18 h, respectively, vs. 12 h for the 10-membered ring), good yields were obtained. All the reactions took place at $-78\text{ }^{\circ}\text{C}$, indicating the reactivity of this system, which was attributed to the single electron transfer (SET) process from indium to the allylic species for the formation of the allyl-indium reagent.

4.2. Substrate chirality-controlled stereoselectivity

On many occasions, pre-existing chiral centers in substrate structures may serve as stereocontrolling elements that direct the outcome of Barbier couplings, especially if found in proximity to the carbonyl center undergoing nucleophilic attack. This is the most frequently encountered scenario in natural product synthesis, where chiral centers in precursor molecules are typically abundant and may participate in conformational regulation (sterically or electronically) as well as chelate formation with the metal mediator of the Barbier reaction, in certain cases. A variety of representative case studies follows, aiming to highlight both the

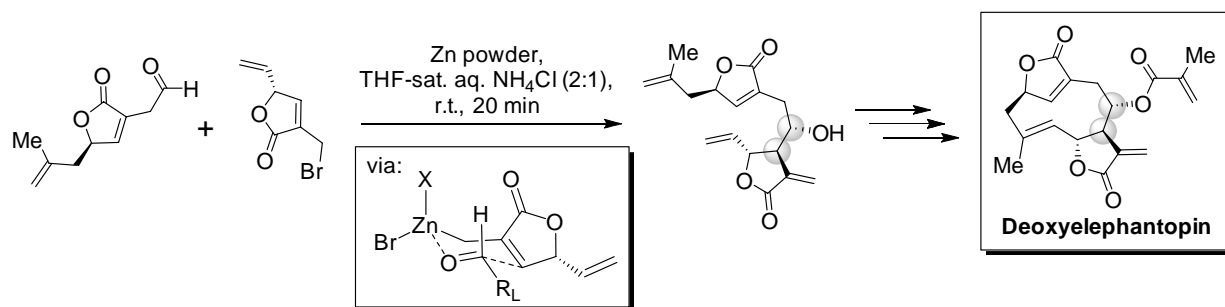
diversity of substrates for Barbier, as well as the numerous factors that have to be considered to rationalize the observed stereochemical outcomes and the models invoked to describe the corresponding transition states.

4.2.1. Deoxyelephantopin

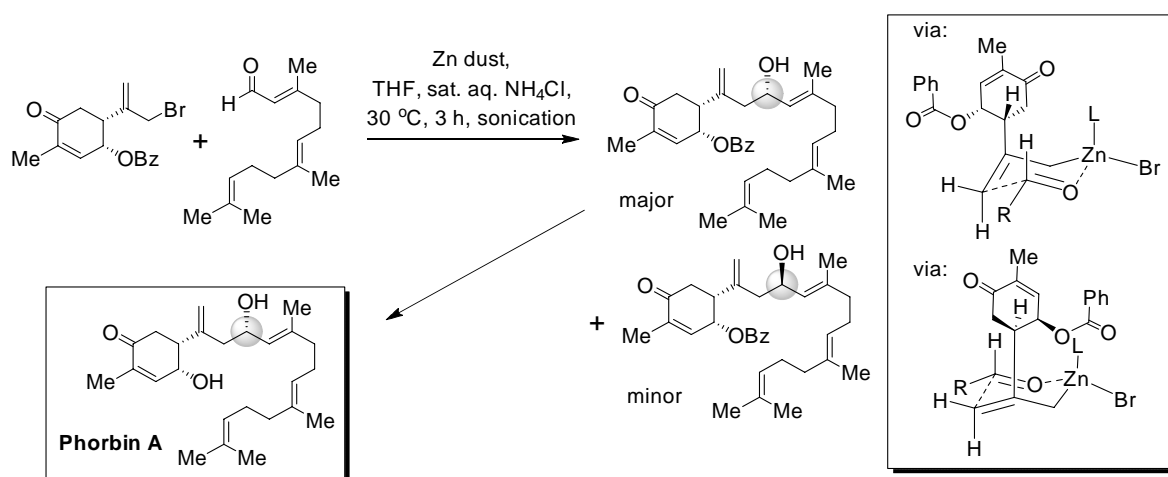
Winssinger and co-workers employed a Zn-mediated Barbier allylation protocol in their synthesis of Deoxyelephantopin analogues, to obtain a key intermediate in a regio- and stereoselective manner (Scheme 22) [111]. In this case, the stereochemical outcome can be rationalized by invoking a Zn-organized 6-membered chair-like (Zimmerman-Traxler) transition state, in which the vinyl group of the allylic component (unsaturated lactone) is facing away from the aldehyde component, in order to avoid unfavorable steric hindrance. In this transition state, the large group on the aldehyde is positioned equatorial.

4.2.2. Phorbin A

In their studies towards the naturally-occurring sesterterpenoid Phorbin A, Brimble and co-workers utilized a similar Zn-mediated Barbier allylation protocol for the connection of farnesal and an allylic *cis*- γ -hydroxycarvone derivative (Scheme 23) [112]. A Zimmerman-Traxler transition state may help explain the observed stereoselectivity. In this case, the bulky chiral 6-membered carvone ring, *via* proximal placement to the organizing metal center, serves as a stereocontrolling element



Scheme 22. Stereocontrolled Zn-mediated Barbier allylation towards the sesquiterpene lactone Deoxyelephantopin [111].



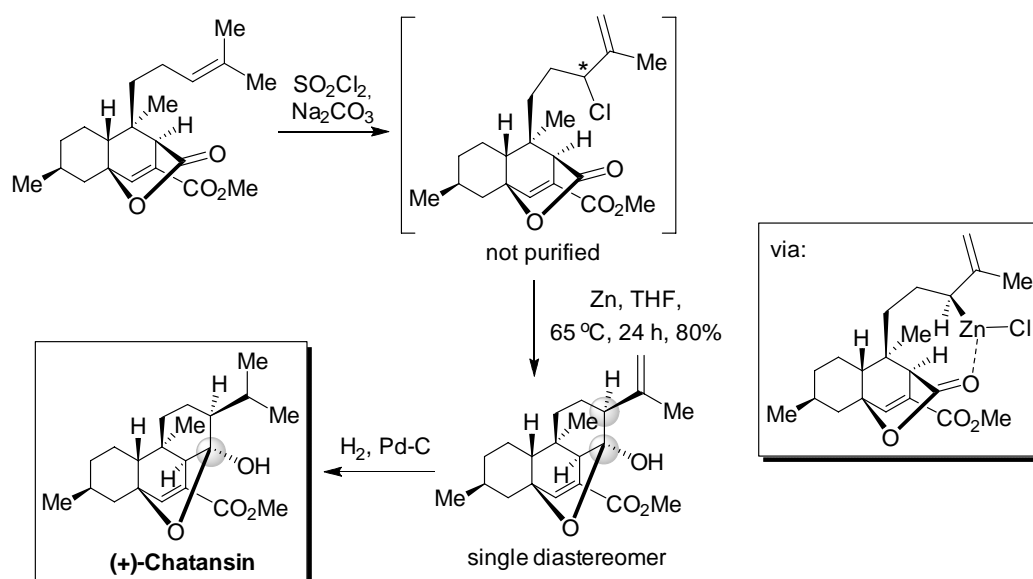
Scheme 23. Zn-mediated Barbier allylation en route to Phorbin A, employing the carvone-derived component as stereocontrolling element [112].

that creates different environments, with regard to steric hindrance, at its two faces. Two alternative transition states of different energy lead to the two observed diastereomers, in different amounts. It is unclear whether the energy differentiation of the two transition states is solely due to different 1,3-diaxial interactions or the benzoyl ester also plays a role in terms of its positioning relative to the Zn-center. The major diastereomer afforded Phorbin A, after ester hydrolysis.

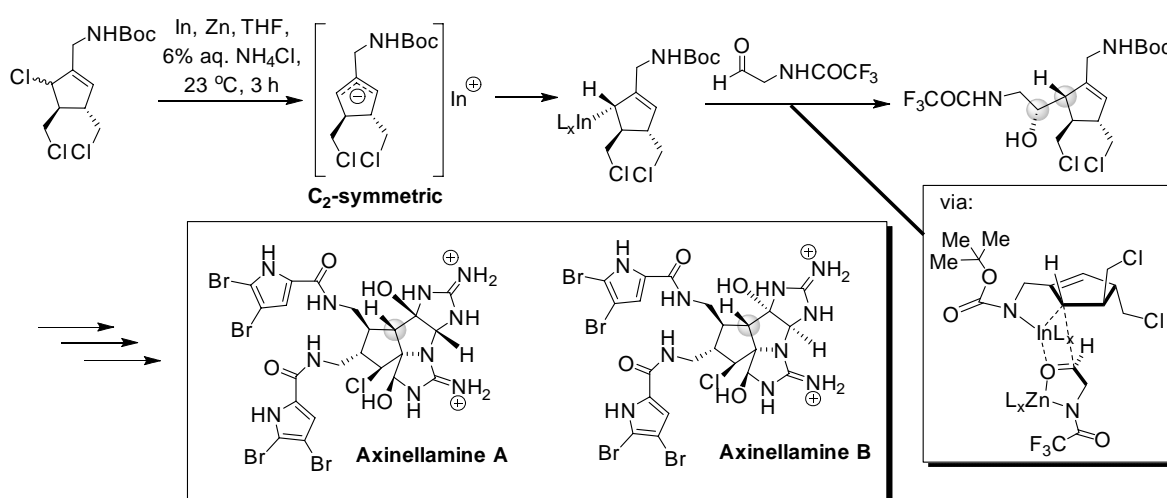
4.2.3. (+)-Chatansin

Maimone and co-workers have described a synthesis of (+)-Chatansin, where an intramolecular Zn-mediated Barbier in THF achieves conversion of a tricyclic advanced intermediate lactone to a tetracyclic lactol product, which after a final

hydrogenation step affords the natural product (Scheme 24) [113]. This is an example of α -position attack of the secondary allyl zinc nucleophile on a lactone carbonyl. The substrate structure controls the stereochemical configuration of the new lactol stereocenter. The lactone precursor is rigid, leaving no alternative to the carbonyl but to undergo attack from the upper face of the lactone ring, especially since the chain containing the allyl zinc has *cis* configuration relative to the lactone bridge. The isolation of only one diastereomer is mentioned, in 80% yield. Given that the substrate used was a mixture of two unseparated diastereomers, with regard to the previous (sulfuryl chloride) step that generated the allyl chloride moiety, it can be deduced that only one of these allyl chlorides contributes to the formation of the desired product.



Scheme 24. A Zn-mediated Barbier reaction involving α -addition of a secondary allyl zinc intermediate on a lactone in THF, was the key step in constructing the full carbon skeleton of (+)-Chatansin [113].



Scheme 25. In/Zn-mediated Barbier allylation en route to Axinellamines A and B [114].

4.2.4. Axinellamines A & B

In their quest for the natural product alkaloids Axinellamines A and B, Baran and co-workers utilized an elegant bimetallic (In/Zn) Barbier coupling for the allylation of an aldehyde using a cyclic allyl chloride (Scheme 25) [114]. The unique structure of this halide component in conjunction with an unprecedented synergistic behavior of the two metals in the Barbier, eliminated multiple

possibilities for alternative products, with regard to regio- and stereocontrol, leading to a single product. Oxidative addition of the metal mediator to the allyl chloride generates a putative allyl-indium intermediate which, due to allyl anion delocalization between the equivalent α - and γ -positions (C_2 -rotational symmetry in the free anion), ensures formation of a single *trans*-configured σ -organometallic species relative to its vicinal alkyl group (CH_2Cl). Once this forms, it is deemed

possible that the Barbier proceeds via α -attack. The inclusion of carbamate (Boc) and amide (COCF_3) moieties in strategic positions in the two substrates implies their involvement in coordinating the metal cations, in a way that restricts free rotation. While unclear which metal is the main mediator for the Barbier, it is possible that both convert to metal cations via initial oxidative addition to the allylic C-Cl bond, and transmetallation events are possible. We propose a plausible transition state in Scheme 25, that takes the above into account as well as the steric hindrance role of the two (*trans*) methylene chloride groups. An alternative γ -attack cannot be excluded.

4.2.5. Cyanolide A

Significant diastereoselectivity (4:1) was observed during the Zn-mediated allylation employed by Bates and Lek for the synthesis of an acetal-based precursor to Cyanolide A (Scheme 26) [115].

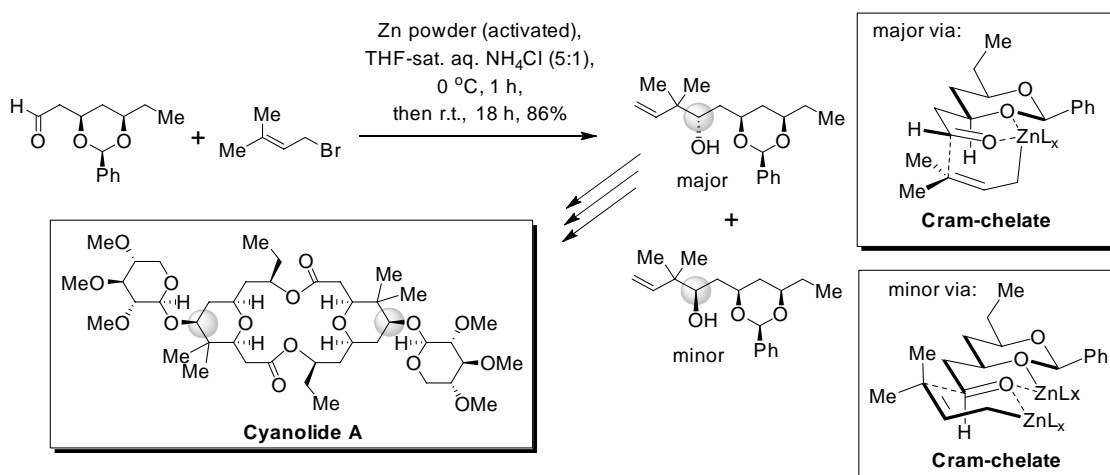
The presence of a β -oxygen atom in this substrate relative to the aldehyde carbonyl provides the possibility for chelate complex formation. In the putative Cram-type chelate model, the upper face of the carbonyl encounters hindrance by the acetal ring. The lower face may allow easier γ -attack to an internal allyl nucleophile, associated with the zinc center, which would also lead to significant torsional strain release and would rationalize the stereo-configuration of the major product. The minor product cannot be produced by an upper

attack from an equatorial allyl nucleophile on the same zinc center; therefore, it would have to come from a second zinc center, from the external face of the chelate complex.

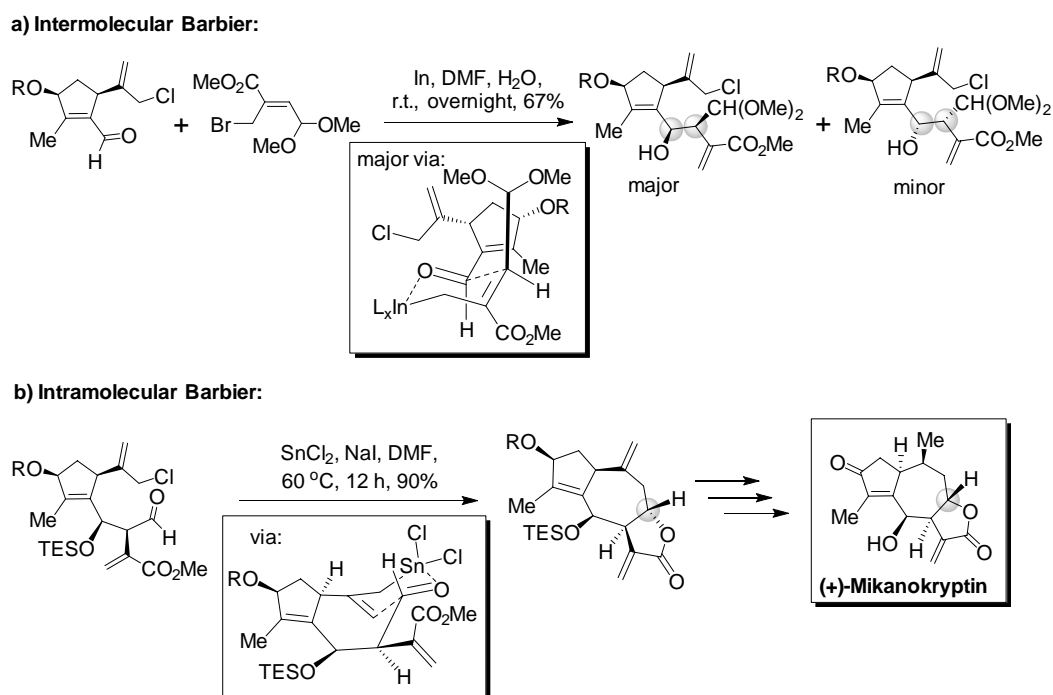
4.2.6. (+)-Mikanokryptin

Maimone and co-workers have highlighted another case where pre-existing chirality in the substrate and ability for chelation of the metal mediator have led to stereocontrol, in their synthesis of (+)-Mikanokryptin. In the same synthesis, they reported both an intermolecular Barbier reaction, mediated by indium, and an intramolecular one mediated by tin chloride (Scheme 27) [116, 117].

With regard to the intermolecular coupling reaction (Scheme 27a), the aldehyde component comprises two stereocenters in *cis* configuration, thus imposing a large steric hindrance to transition state formation on that face. Instead, attack from the nucleophilic allyl indium species will preferentially occur from the opposite face of the 5-membered ring, leading to the major product depicted above, provided that the 5-membered ring is positioned equatorial in the Zimmerman-Traxler transition state. The diastereomeric excess was 2:1, indicating that the steric hindrance does not entirely exclude an alternative transition state, with the aldehyde placed in front of the nucleophile and the 5-membered ring rotating to position the methyl group proximal to the aldehyde O atom. A



Scheme 26. Zn-mediated Barbier allylation employed in the synthesis of Cyanolide A, and proposed transition states for the major and minor product [115].



Scheme 27. In- and Sn-mediated Barbier allylations towards (+)-Mikanokryptin [116].

noticeable feature of this protocol is the complete chemoselectivity, where only the allyl bromide reacts with the carbonyl, despite the presence of an allyl chloride in the structure. This is indicative of the increased reactivity of the allyl bromide substrates towards oxidative metalation compared to allyl chlorides.

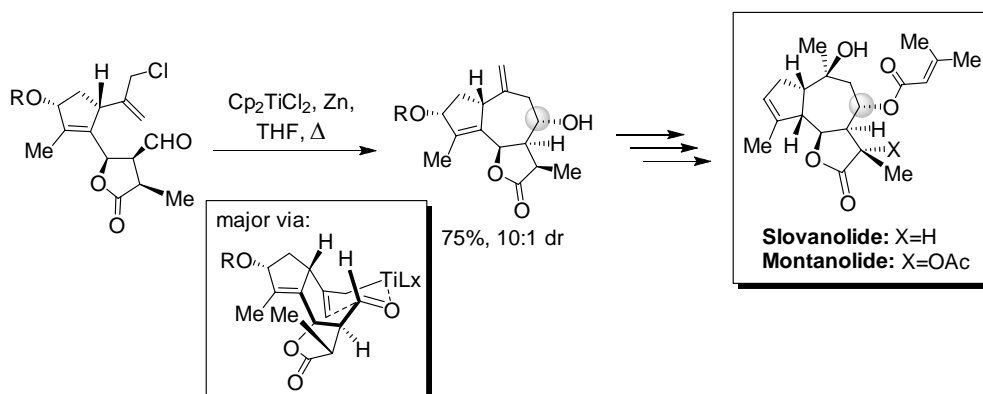
In the intramolecular Barbier allylation (Scheme 27b), the intermediate-size cyclic transition state and the high strain in the system, due to the presence of double bonds, dictates the way in which the transition state is organized around the strongly Lewis acidic metal center, leading to a single product with no other observed diastereomer, which undergoes spontaneous lactonization. The low reactivity of the allyl chloride towards this type of reaction is circumvented by means of a Finkelstein reaction that generates the corresponding allyl iodide *in situ*.

4.2.7. Slovanolide, Montanolide, Nortrilobolide

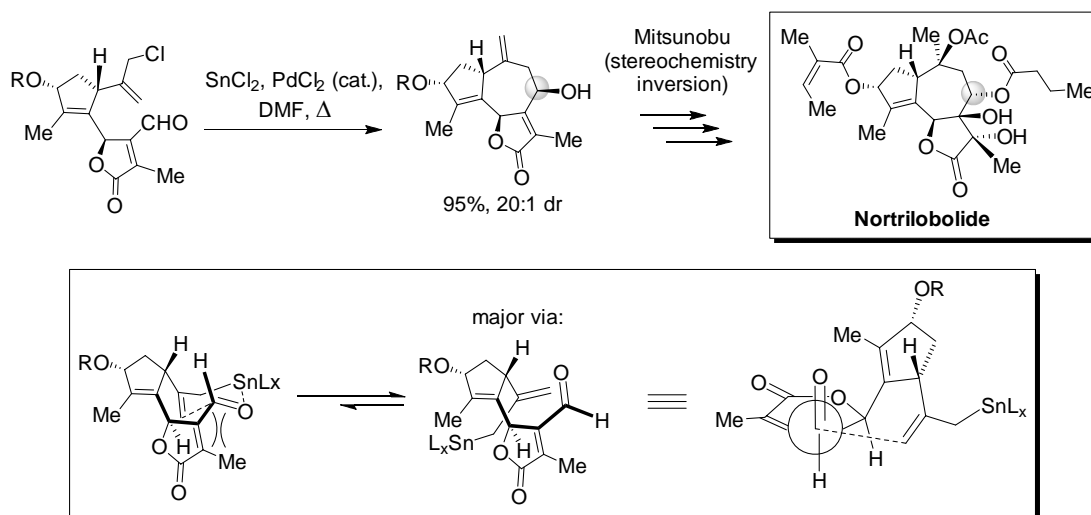
To access structurally related natural products with similar [5,7]-ring carbon frame as Mikanokryptin, but different positioning of the 5-membered lactone, Maimone's research team

have also applied a titanocene/Zn Barbier protocol on a bifunctional precursor that contains the pre-formed lactone (Scheme 28). Again, the constrained transition state dictates the stereochemical configuration, by means of a Zimmerman-Traxler complex. The organizing role of the titanocene is important in this case for achieving high diastereoselectivity (10:1). The generated chiral center is employed as a OH handle at a later stage in the synthesis to attach an acyl group, present in the final products, Slovanolide and Montanolide [117].

Interestingly, for a Barbier reaction on a very similar substrate with higher degree of unsaturation (one additional double bond in the lactone ring), the transition state in Scheme 28 appears to be destabilized, likely due to a steric clash of the now planar lactone ring on the intramolecular allylic nucleophile or due to increase of rigidity in the system that prevents it from reaching a chair-like transition state. Destabilization of the chair-like complex could cause the reaction to proceed via non-Zimmerman-Traxler transition state, resulting in opposite stereoconfiguration. In this case, the authors employed a SnCl_2 protocol, with catalytic PdCl_2 in DMF (Scheme 29) [117].



Scheme 28. Titanocene/Zn Barbier protocol employed to generate a tricyclic system *via* intramolecular allylation in the synthesis of natural products Slovanolide and Montanolide [117].



Scheme 29. $\text{SnCl}_2/\text{PdCl}_2$ Barbier protocol employed to generate a tricyclic system *via* intramolecular allylation in the synthesis of natural product Nortrilobolide [117].

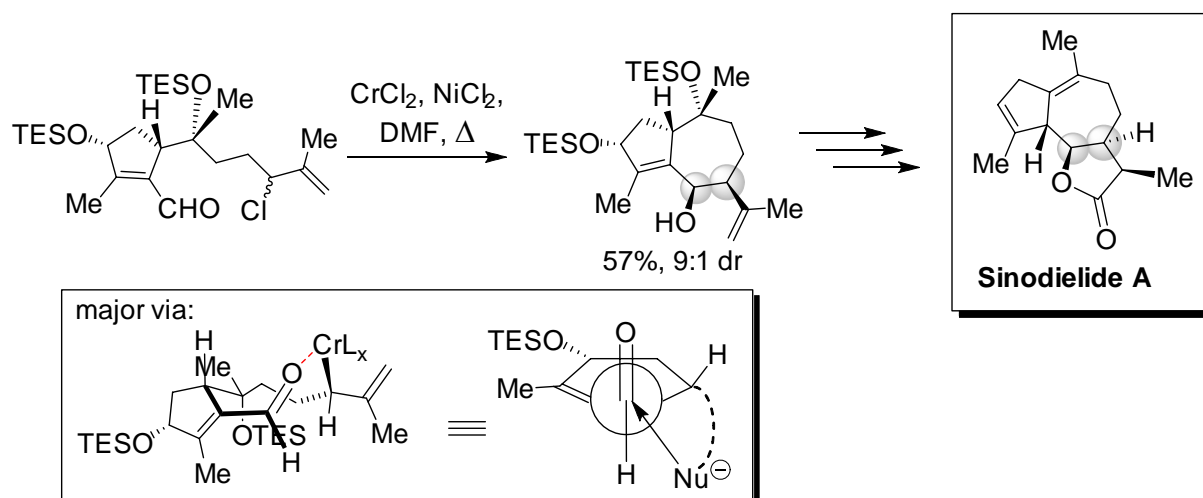
4.2.8. Sinodiellide A

By applying a Cr/Ni-mediated NHK protocol, Maimone and co-workers achieved the diastereoselective intramolecular attack of a secondary allylic nucleophile on an aldehyde, leading to the assembly of a related fused [5,7]-ring system, precursor to the natural product Sinodiellide A (Scheme 30) [117]. A 9-membered complex formed from coordination of the chromium on the carbonyl is likely to be responsible for guiding the allyl nucleophile to conduct α -attack *via* a Bürgi-Dunitz angle, while at the same time minimizing sterics (i.e., placing Me and isopropene substituents pseudo-equatorial). Having an opposite

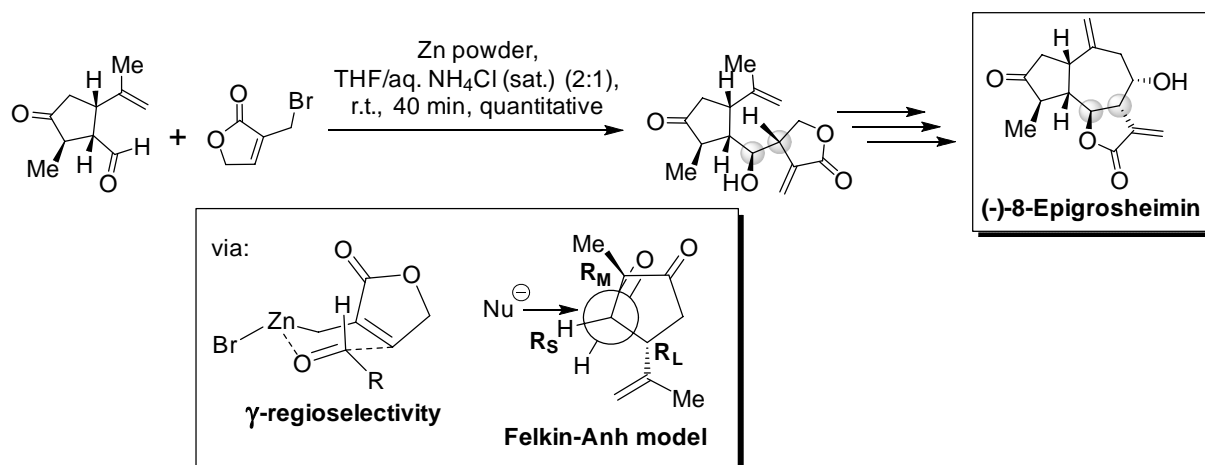
stereoconfiguration at the allyl chloride α -position would position the isoprene group against the aldehyde, destabilizing the metal-organized complex. This is presumably the reason for the lower reactivity of the diastereomeric chloride, which accounts only for 1/10th of total product formation.

4.2.9. (-)-8-Epigrosheimin

During their synthetic studies towards the natural product (-)-8-Epigrosheimin, Xu and co-workers applied an intermolecular Zn-mediated Barbier reaction involving the bromide of an unsaturated lactone (Scheme 31) [118]. This protocol allowed for quantitative transformation, while at the same



Scheme 30. A stereoselective variation of the NHK reaction (Cr/Ni-mediated) was employed as a key step in the generation of a bicyclic system *via* intramolecular secondary allyl nucleophile attack on aldehyde, in the synthesis of Sinodielide A [117].

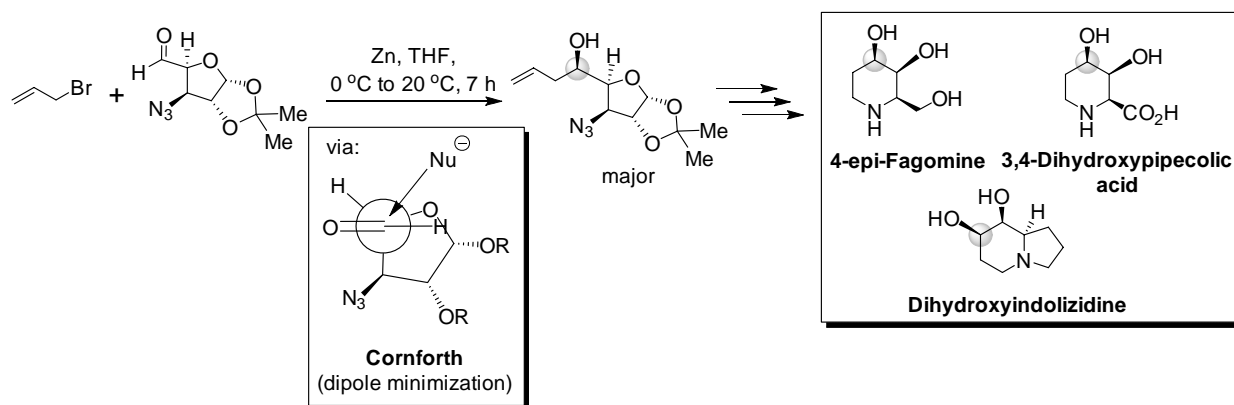


Scheme 31. Zn-mediated Barbier allylation towards (-)-8-Epigrosheimin [118].

time being highly chemoselective, since the ketone moiety remained unreactive, and completely regio- and stereoselective, since the desired γ -*anti* product was the only one observed. The stereochemical outcome can be rationalized by means of a Felkin-Anh transition state, with the largest α -substituent (isoprenyl-substituted carbon) placed perpendicular to the carbonyl and the smallest α -substituent (H) oriented away from the carbonyl oxygen, as to allow for an unhindered attack via a Bürgi-Dunitz trajectory.

4.2.10. Natural product analogues 4-Epi-Fagomine, 3,4-Dihydroxypipelic acid, Dihydroxyindolizidine

An interesting example of stereocontrolled Barbier reaction, highlighting the strong influence of a polar α -substituent, was reported by Chattopadhyay and co-workers, as part of their synthesis of various non-natural structural analogues of natural products Fagomine and Pipelic acid [119]. The reaction employed Zn as the metal and took place in THF, leading to 95:5 diastereomeric ratio in favor of the depicted (major) product (Scheme 32).



Scheme 32. Zn-mediated Barbier allylation of a furanose aldehyde in THF, part of the synthesis of 4-epi-Fagomine, 3,4-Dihydroxypipicolinic acid and Dihydroxyindolizidine. Lack of chelation leads to an open transition state, involving sterics and dipole minimization [119].

Noticeably, the major product cannot be rationalized in terms of a Cram-type chelate model. One has to invoke a modified Cornforth model, involving an open transition state where the two O atoms (the carbonyl and furanose ring oxygen) are oriented in opposite directions in order to minimize dipole repulsion. Also, sterics from the azide-substituted carbon of the sugar are kept at a minimum. This model assumes a weak, non-stable zinc chelate with the furanose ring oxygen and carbonyl in THF. In fact, this notion is supported by a previous report by Danishefsky and co-workers, which mentions a dihedral angle between the C=O and C-O bonds in a similar xylose-derived system to be 157.4° [120], compatible with the Cornforth-predicted configuration of the transition state.

4.2.11. Cochliomycin C, Paecilomycin F, (3R,4S)-4-Hydroxylasiodiplodin, Verbalactone, Stagonolide C, (-)-Cleistenolide, (+)- β -Conhydrine

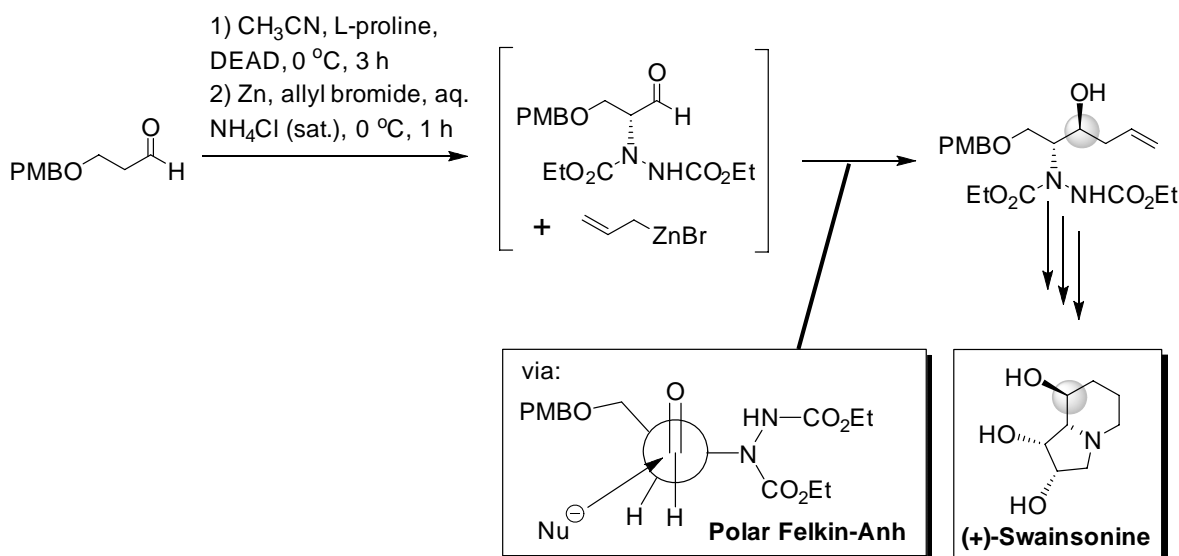
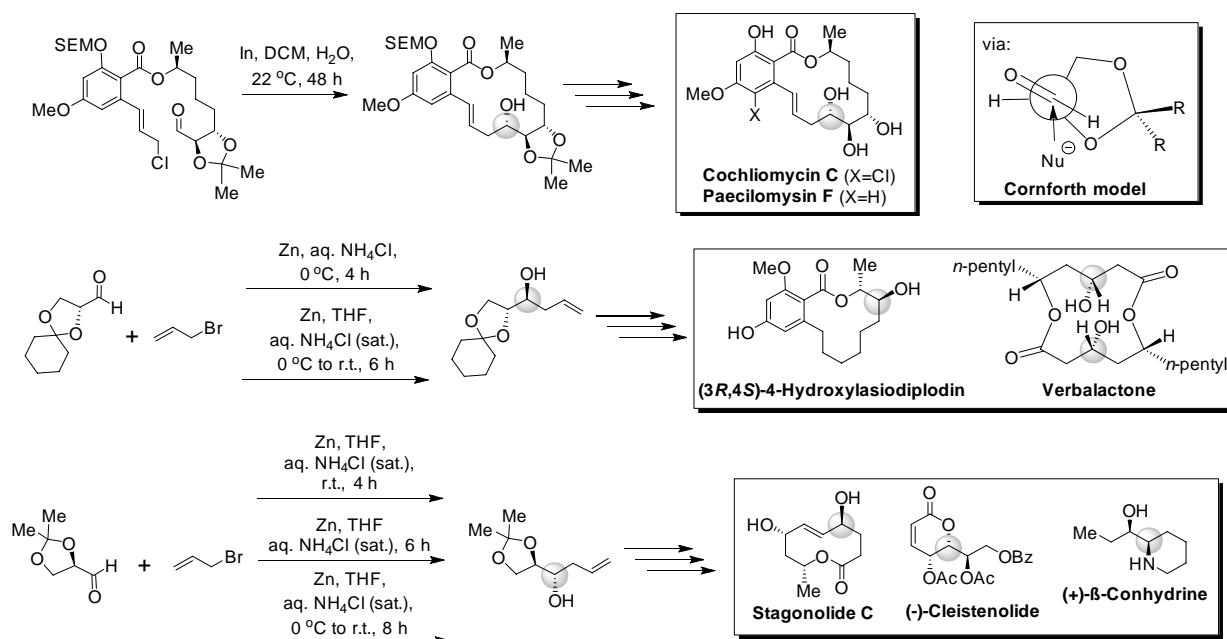
Several similar examples of Barbier reactions that proceed with considerable stereocontrol exhibit an α -oxygen substituent, part of a vicinal diol protected as a ketal (Scheme 33) [121-126]. All these cases involve Zn-mediated or In-mediated protocols in aqueous systems, where chelate formation would normally be a favored option. However, the stereochemical outcome can only be explained by invoking the Cornforth model, which emphasizes the dominant effect of dipole repulsions, as was the case in the previous example.

4.2.12. (+)-Swainsonine

A chiral α -hydrazinoaldehyde, generated *in situ* by means of L-proline catalysis from an achiral aldehyde precursor and diethyl azodicarboxylate (DEAD), served as the starting material towards the synthesis of (+)-swainsonine (Scheme 34) [127]. Addition of Zn, allyl bromide and a saturated aqueous solution of NH_4Cl to the reaction, led to stereocontrolled Barbier allylation, guided by the pre-existing stereocenter. The authors suggest a Felkin-Anh transition state to rationalize the observed stereoconfiguration. Chelate complex formation, either with the PMB ether oxygen or the distal nitrogen atom appears to be disfavored in this acetonitrile-water solvent system. This example showcases the effect of steric volume, with the branched hydrazine substituent placed antiperiplanar to the incoming nucleophile, leading to an impressive 99:1 d.r.

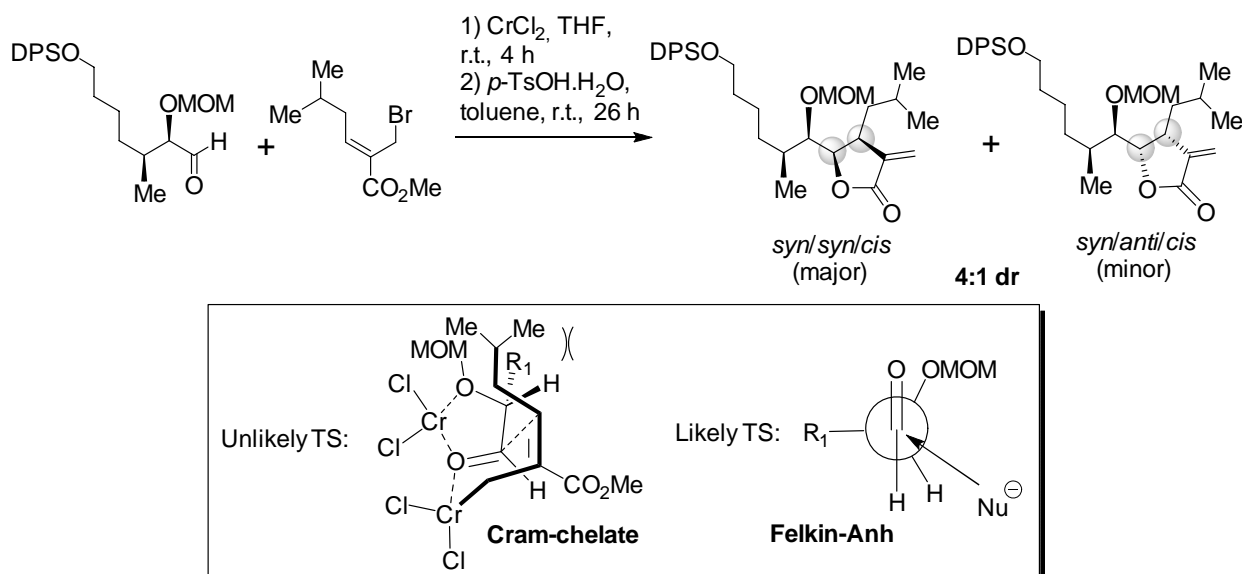
4.2.13. Uprolide D analogue

A very interesting example was reported by Marshall *et al.* in the context of their studies towards the cembranolide Uprolide D [128], which employed an allylation protocol mediated by CrCl_2 in THF, in the presence of *p*-TsOH, to induce lactonization after the coupling. In this case, an intermolecular model substrate system and an intramolecular substrate system afforded different diastereoselectivity preference, suggesting a dual mechanistic pathway.



In the intermolecular model system, the major product was found to be a *syn/syn/cis* lactone, forming in 4:1 dr relative to the minor product, the *syn/anti/cis* lactone (Scheme 35). While the occurrence of the major product could be explained by invoking a Cram-chelate model that involves coordination of both the carbonyl oxygen

and the MOM ether oxygen on Cr(II), and delivery of the allyl chain from the less hindered face of the chelate complex, this was deemed unlikely by the authors. This case differs from other cases examined in this review, since the allylic species contains a *Z* alkene instead of an *E* alkene. For the *Z* alkene to engage in a Zimmerman-Traxler-type

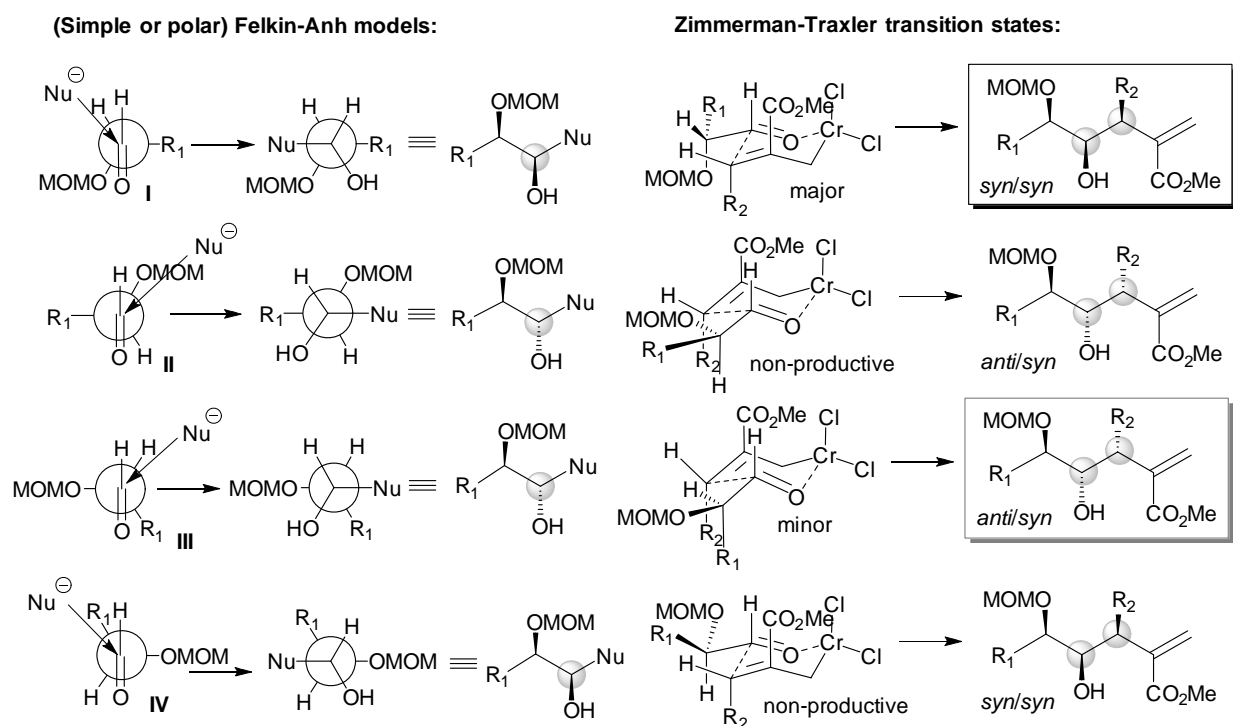


Scheme 35. Cr-mediated Barbier-type allylation towards an Uprolide D diastereomer, indicating unlikely and likely transition states [128].

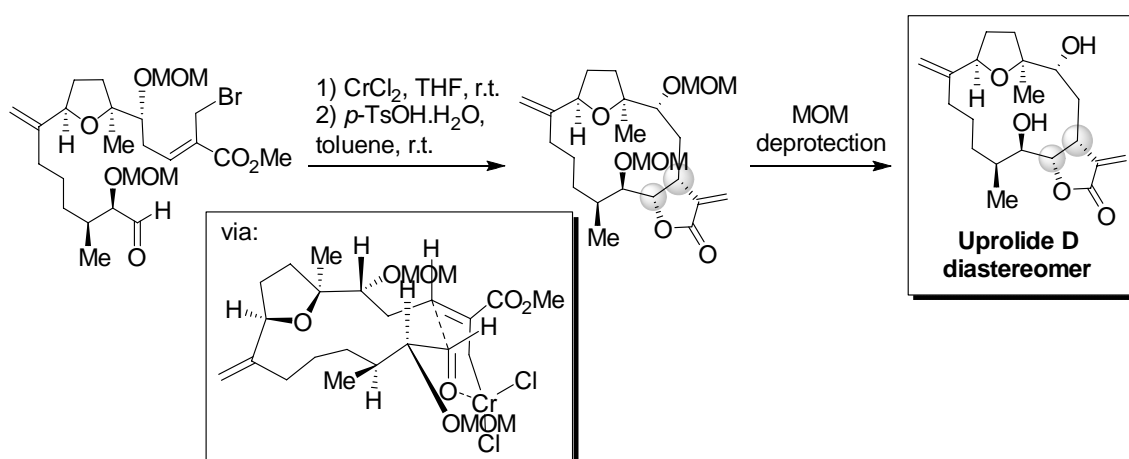
transition state with the carbonyl, it would have to suffer a disfavored steric interaction between its own isobutyl substituent and the chelation complex. Therefore, while a Cram-chelate complex correctly predicts the major product, it is unlikely to be in play. The classic Felkin-Anh model needs to be invoked to explain the observed stereochemistry.

A comparison of various rotamers of the aldehyde substrate (Scheme 36) may explain why the one represented in Scheme 35 is thought to be the preferred one for reaction. Rotamers II and IV block the trajectory of the incoming chromium nucleophile by positioning a large substituent (OMOM or the branched R_1 , respectively) directly in its path, preventing the organization of the corresponding transition states. The remaining two rotamers, I and III, believed to lead to the major and minor diastereomer, respectively, are more favorable for allowing organization of a transition state. Out of these two, rotamer I suffers from dipole repulsion between oxygen atoms and minor sterics from approaching the O atom of MOMO and R_2 ; however, this is not as detrimental as a steric clash between branched R_1 and R_2 , encountered in the case of rotamer III-derived transition state. The transition state related to rotamer I is a classic Felkin-Anh, while the one related to rotamer III is a polar Felkin-Anh.

The same protocol was employed in the intramolecular variant of the reaction, leading to macrocyclization, but this time producing a single diastereomer [128]. Although in the intermolecular reaction the *syn/syn/syn* intermediate was the major one and the *syn/anti/syn* was the minor, in this case the stereoselectivity is reversed in favor of the *syn/anti/syn* intermediate, which is the only one observed. The synthesis was concluded by converting this intermediate to an Uprolide D diastereomer (*syn/anti/cis*) rather than the natural product itself (*syn/syn/cis*) (Scheme 37). This can be attributed to the size and nature of the tether connecting the aldehyde and bromide groups in the substrate, which restricts the relative orientation of nucleophile and electrophile, while at the same time the substrate assumes a conformation that minimizes transannular strain in the transition state and positions all large substituents (Me and two OMOM groups) pseudo-equatorial (Scheme 37). Therefore, an antiperiplanar attack of the nucleophile relative to the large carbon substituent of the α -position (simple Felkin-Anh model) is restricted in this case, in contrast to the intermolecular counterpart. Instead, the incoming nucleophile attacks anti-periplanar to the OMOM group, in a way reminiscent of the transition state leading to the minor product of the intermolecular example. This mode of attack rationalizes the formation of



Scheme 36. (Simple and polar) Felkin-Anh models considered to rationalize the stereochemical outcome of the reaction of Scheme 35, and corresponding Zimmerman-Traxler transition states showing intermediate homoallylic alcohols.



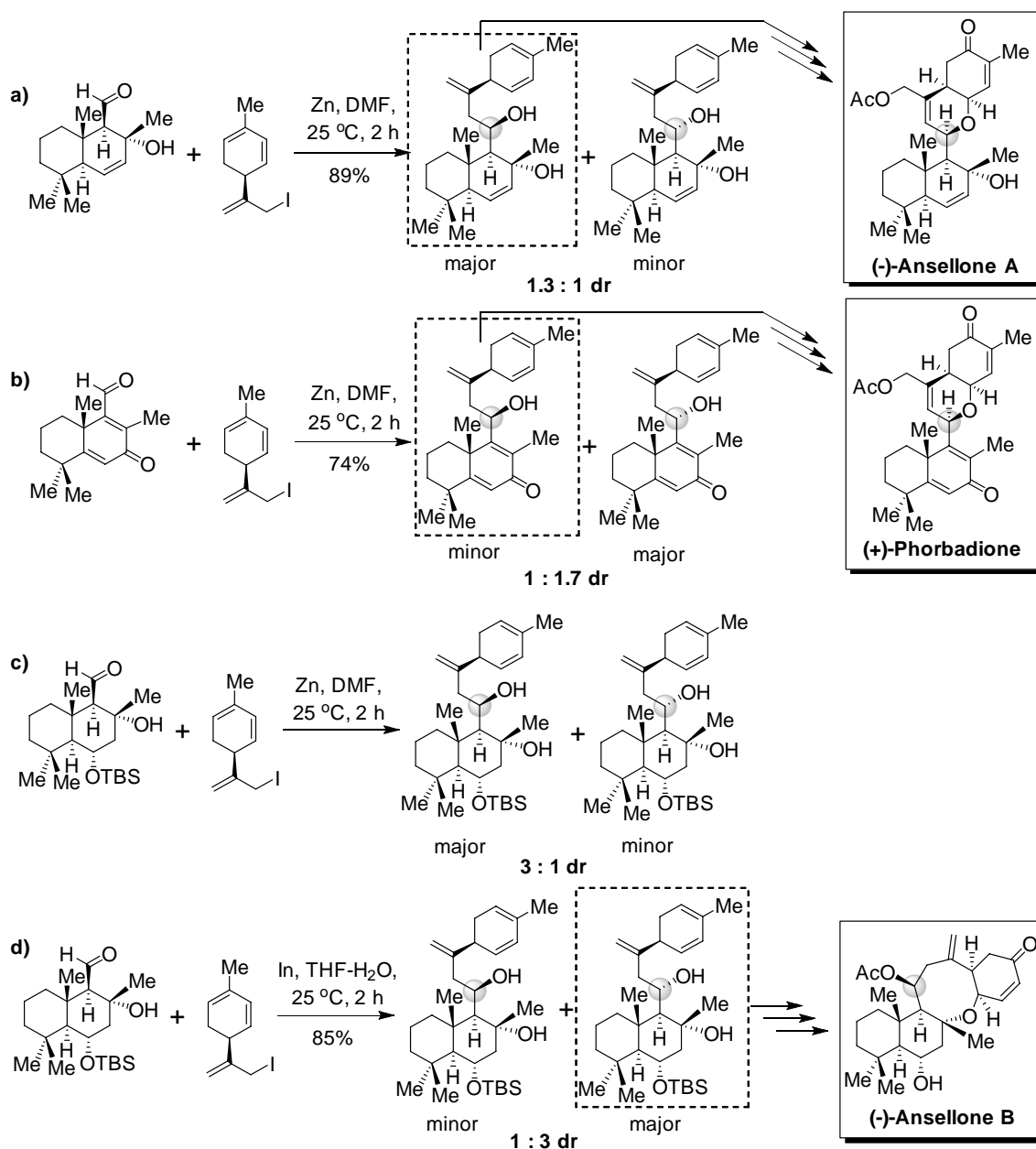
Scheme 37. Cr-mediated Barbier-type allylation/macrocyclization towards an Uprolide D diastereomer [128].

a *syn/anti/syn* intermediate, which is eventually observed in the form of the *syn/anti/cis* lactone as the major final product.

4.2.14. (-)-Ansellones A and B, (+)-Phorbadiene

Zn- and In-mediated Barbier allylation protocols

were employed on 3 related substrates in a recent study by Tong and co-workers for the synthesis of sestertepenoic structures Ansellone A, Ansellone B and Phorbadiene [129], affording good yields and various levels of diastereoselectivity. The observed diastereoselectivity ratios reflect the



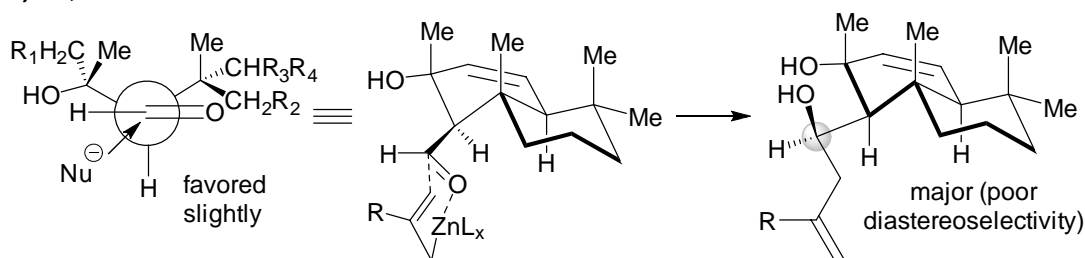
Scheme 38. Barbier allylation reactions employed in a study towards (-)-Ansellone A, (-)-Ansellone B and (+)-Phorbadiene. The diastereomer further progressed in the synthesis to afford each natural product is highlighted in dotted frame [129].

complexity of the substrate structures and the diverse controlling factors in play. The investigated cases are shown comparatively in Scheme 38 below.

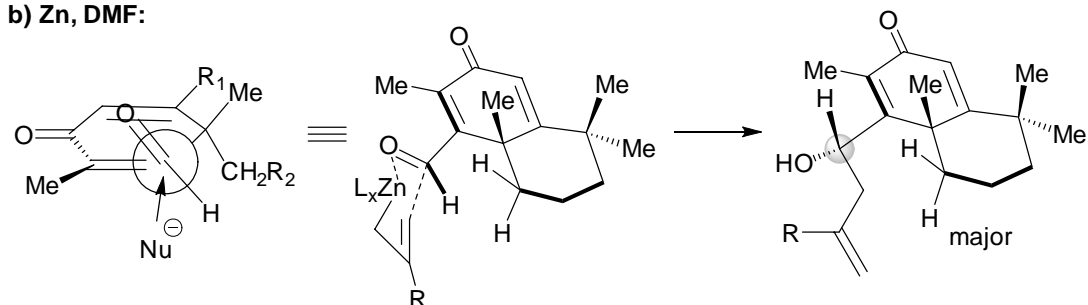
The bicyclic substrate of reaction (a) (Scheme 38), comprising one endocyclic double bond, leads to the lowest diastereoselectivity (1.3:1 dr) under Zn/DMF conditions, with the major product not

being derived from a chelate-mediated pathway. In this case, a dipole-minimization model could explain the occurrence of the major product (Scheme 39a). However, given the torsion imposed on the unsaturated 6-membered ring by the presence of the double bond, the OH substituent is positioned at a distance from the aldehyde carbonyl

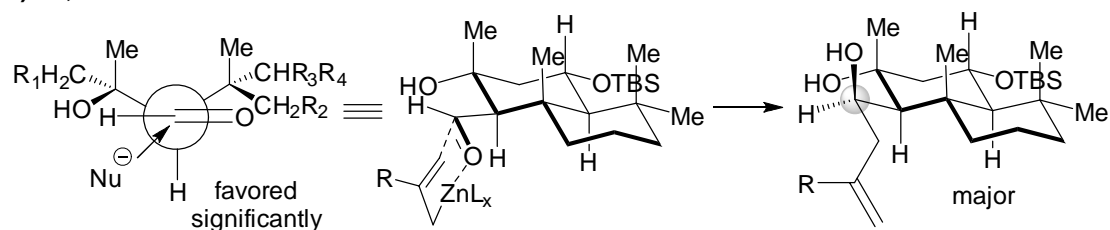
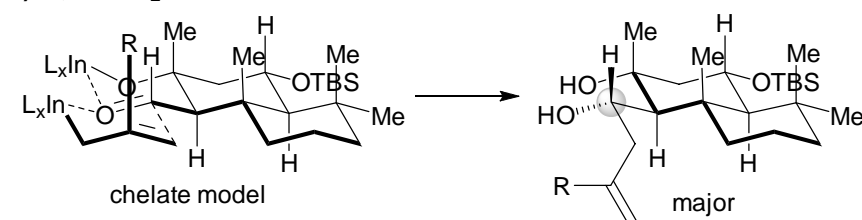
a) Zn, DMF:



b) Zn, DMF:



c) Zn, DMF:

d) In, THF-H₂O:

Scheme 39. Proposed transition states to explain diastereoselectivity outcomes for the four (4) Barbier cases shown in Scheme 38.

group, and hence the effect of dipole repulsion would be expected to be weak. Simple rotation of the carbonyl would afford a different conformer of slightly higher energy, responsible for the minor product. The transition state is likely organized on the lower face of the carbonyl, to avoid steric hindrance with the ring's axial substituents. The major product was converted to (-)-Ansellone A.

A different scenario is faced with the more unsaturated substrate of reaction (b) (Scheme 38),

which is nearly planarized due to the presence of two C=C bonds and a C=O bond. In this case the two carbonyl dipoles are isolated and the steric bulk imposed by the two β -positions (sp^2 vs. sp^3) relative to the aldehyde carbonyl is different. Under the same conditions (Zn/DMF), the proposed non-chelate transition state (Scheme 39b) may allow for a Bürgi-Dunitz trajectory for the zinc nucleophile from the lower face of the carbonyl in the conformer shown, while alleviating sterics as

well as $A_{1,3}$ strain. In this case the diastereoselectivity ratio is 1.7:1, in favour of the major product, which now has opposite stereochemical configuration, compared to that of reaction (a). However, the required stereoconfiguration for the natural product (+)-Phorbadiolone was that of the minor product, which was carried through in the synthesis.

Improved stereocontrol (3:1 dr) was achieved with Zn/DMF with the substrate of reaction (c) (Scheme 38), where the bicyclic carbon frame is fully saturated. While the major product's stereochemical configuration suggests a non-chelating pathway, as was the case in reaction (a), the same factors that played a role in reaction (a) likely have a stronger impact here. Due to ideal tetrahedral angles, the positioning of the OH and C=O dipoles is now more proximal compared to the partially unsaturated substrate of reaction (a); hence a stronger dipole repulsion is expected to increase the preference for the proposed rotamer, which alleviates this repulsion (Scheme 39c). However, the stereoconfiguration of the main product was not the desired one for progressing it to (-)-Ansellone B, creating a need for a different protocol to be introduced.

By applying In-mediated conditions on the fully saturated substrate used in the previous reaction, in THF-water (Scheme 38d), a Cram chelate transition state can presumably assemble. This locks the OH and C=O oxygen atoms in parallel, allowing nucleophile attack on the carbonyl from the outer side, since the back side of the transition state complex is blocked by the ring system (Scheme 39d). Importantly, the stereoconfiguration is switched relative to reaction (c), affording the desired diastereomeric homoallylic alcohol derivative for the construction of (-)-Ansellone B.

5. Conclusions and outlook

The Barbier reaction, in its numerous diverse variants, has provided a powerful and often irreplaceable synthetic tool for the construction of chiral homoallylic alcohols. A large number of protocols are now available, that address issues of chemical compatibility with pre-existing functional groups, air sensitivity of the organometallic species, substrate solubility, chemical reactivity

(of both substrate and metal-mediator) and the fine-tuning of reactivity, development of catalytic vs. stoichiometric processes, as well as "green chemistry" considerations.

On the issue of selectivity, appropriately designed substrates and conditions can be selected to achieve high levels of chemoselectivity (aldehydes more reactive than ketones, allyl halides exhibiting increasing reactivity in the order chlorides < bromides < iodides), regioselectivity (α - vs. γ - attack of the allylic nucleophilic species to the carbonyl) and enantio- or diastereoselectivity. Stereoselectivity can be controlled by means of chiral additives/ligands/auxiliaries added to the reaction mix, or by simply relying on substrate pre-existing stereochemistry, to direct the Barbier coupling's stereochemical outcome. Both approaches have been successfully implemented in the context of natural product synthesis, with many examples of homoallylic alcohol-comprising natural products and analogues having been reported in recent years.

Through these studies, the diverse and often contradicting factors controlling the stereoconfiguration of the generated chiral centers are becoming better understood, and encompass, more noticeably, sterics, electronics (i.e., dipole repulsions), ability (or lack thereof) of the substrates to form chelates under reaction conditions, torsional and transannular strain in small- and medium-size transition states, and the solid requirement of the system for nucleophilic attack following an acceptable trajectory.

In many aspects, the Barbier reaction remains unmatched and relatively more versatile in comparison to many other coupling methods and, therefore, is expected to continue to be a method of choice in the following years, for the construction of the valuable homoallylic alcohol motif in natural products, analogues and other useful structures. More challenging substrate systems are expected to be tested and to provide an updated picture of the power of the Barbier transformation as a tool for the construction of complex molecular architectures.

CONFLICT OF INTEREST STATEMENT

The authors declare no conflict of interest.

REFERENCES

1. Barbier, P. 1899, *C. R. Hebd. Acad. Sci.*, 128, 110.
2. Grignard, V. 1900, *C. R. Hebd. Acad. Sci.*, 130, 1322.
3. Kang, H. -Y. and Song, S. -E. 2000, *Tetrahedron Lett.*, 41, 937.
4. Kim, S. H. and Han, E. -H. 2000, *Tetrahedron Lett.*, 41, 6479.
5. Kim, S. H., Lee, H. S., Kim, K. H. and Kim, J. N. 2009, *Tetrahedron Lett.*, 50, 1696.
6. Kim, S. H., Lee, H. S., Kim, K. H. and Kim, J. N. 2009, *Tetrahedron Lett.*, 50, 6476.
7. Rizzo, A. and Trauner, D. 2018, *Org. Lett.*, 20, 1841.
8. Maynard, G. D. 2001, 1,2-Dibromoethane. In *Encyclopedia of Reagents for Organic Synthesis*, Paquette, L. A., Crich, D., Fuchs, P. L., Molander, G. A. (Eds), John Wiley & Sons, Inc.
9. Borisov, V. A., D'yachenko, A. N. and Kraidenko, R. I. 2012, *Russ. J. Inorg. Chem.*, 57, 499.
10. Li, C. -J. and Zhang, W. -C. 1998, *J. Am. Chem. Soc.*, 120, 1902.
11. Zhang, W. -C. and Li, C. -J. 1999, *J. Org. Chem.*, 64, 3230.
12. Sormunen, G. J. and Lewis, D. E. 2004, *Synth. Commun.*, 34, 3473.
13. Yuan, S. -Z and Liu, J. 2008, *Chin. J. Chem.*, 26, 804.
14. Zhou, J. -Y., Jia, Y., Sun, G. -F. and Wu, S. -H. 1997, *Synth. Commun.*, 27, 1899.
15. Resende, G. O., Aguiar, L. C. S. and Antunes, O. A. C. 2005, *Synlett*, 1, 119.
16. Balasubramanyam, P. and Rodríguez, A. D. 2017, *Tetrahedron*, 73, 1283.
17. Chowhan, R. L., Reddy, S. M. and Kumar, S. N. 2017, *J. Chem. Sci.*, 129, 1205.
18. Keltjens, R., Vadivel, S. K., de Gelder, R., Klunder, A. J. H. and Zwanenburg, B. 2003, *Eur. J. Org. Chem.*, 2003, 1749.
19. Zhao, L. M., Xu, D. F., Zhou, W. and Li, S. S. 2008, *Lett. Org. Chem.*, 5, 234.
20. Zhao, L. -M., Jin, H. -S., Wan, L. -J. and Zhang, L. -M. 2011, *J. Org. Chem.*, 76, 1831.
21. Wang, Z., Yuan, S. and Li, C. -J. 2002, *Tetrahedron Lett.*, 43, 5097.
22. Araki, S., Ito, H. and Butsugan, Y. 1988, *Appl. Organometallic Chem.*, 2, 475.
23. Andrews, P. C., Peatt, A. C. and Raston, C. L. 2004, *Tetrahedron Lett.*, 45, 243.
24. Wang, J., Yuan, G. and Dong, C. -Q. 2004, *Chem. Lett.*, 33, 286.
25. Bian, Y. -J., Zhang, J. -Q., Xia, J. -P. and Li, J. -T. 2006, *Synth. Commun.*, 36, 2475.
26. Cravotto, G., Gaudino, E. C. and Cintas, P. 2013, *Chem. Soc. Rev.*, 42, 7521.
27. Domini, C. E., Álvarez, M. B., Silbestri, G. F., Cravotto, G. and Cintas, P. 2017, *Catalysts*, 7, 121.
28. Wu, S., Li, Y. and Zhang, S. J. 2016, *Org. Chem.*, 81, 8070.
29. Zhang, F., Wang, R., Wu, S., Wang, P. and Zhang, S. 2016, *RSC Adv.*, 6, 87710.
30. Zhang, M., Jia Y., Zhou, J. and Wu, S. 1998, *Heteroatom Chem.*, 9, 475.
31. Nair, V. and Jayan, C. N. 2000, *Tetrahedron Lett.*, 41, 1091.
32. Imai, T. and Nishida, S. 1993, *Synthesis*, 395.
33. Houlemare, D., Outurquin, F. and Paulmier, C. 1997, *J. Chem. Soc., Perkin Trans. 1*, 1629.
34. Zhou, Y., Zha, Z., Zhang, Y. and Wang Z. 2008, *ARKIVOC*, 2008, 142.
35. Imai, T. and Nishida, S. 1994, *J. Chem. Soc., Chem. Commun.*, 277.
36. Kalita, P. K. and Phukan, P. C. R. 2013, *Chimie*, 16, 1055.
37. Kundu, A., Prabhakar, S., Vairamani, M. and Roy, S. 1997, *Organometallics*, 16, 4796.
38. Debroy, P. and Roy, S. J. 2003, *Organometallic Chem.*, 675, 105.
39. Tan, X. -H., Hou, Y. -Q., Huang, C., Liu, L. and Guo, Q. -X. 2004, *Tetrahedron*, 60, 6129.
40. Tan, X. -H., Shen, B., Deng, W., Zhao, H., Liu, L. and Guo, Q. -X. 2003, *Org. Lett.*, 5, 1833.
41. Chaudhuri, M. K., Dehury, S. K. and Hussain, S. 2005, *Tetrahedron Lett.*, 46, 6247.
42. Tan, X. -H., Hou, Y. -Q., Liu, L. and Guo, Q. -X. 2004, *Chin. J. Chem.*, 22, 450.

43. Tan, X. -H., Tao, C. -Z., Hou, Y. -Q., Luo, L., Liu, L. and Guo, Q. -X. 2005, *Chin. J. Chem.*, 23, 237.
44. Sinha, P. and Roy, S. 2001, *Chem. Commun.*, 1798.
45. Sinha, P. and Roy, S. 2004, *Organometallics*, 23, 67.
46. Rosales, A., Oller-López, J. L., Justicia, J., Gansäuer, A., Oltra, J. E. and Cuerva, J. M. 2004, *Chem. Commun.*, 2628.
47. Sancho-Sanz, I., Miguel, D., Millán, A., Estévez, R. E., Oller-López, J. L., Álvarez-Manzaneda, E., Robles, R., Cuerva, J. M. and Justicia, J. J. 2011, *Org. Chem.*, 76, 732.
48. Steurer, S. and Podlech, J. 2001, *Adv. Synth. Catal.*, 343, 251.
49. Augé, J., Lubin-Germain, N. and Thiaw-Woaye, A. 1999, *Tetrahedron Lett.*, 40, 9245.
50. Augé, J., Lubin-Germain, N., Marque, S. and Seghrouchni, L. J. 2003, *Organometallic Chem.*, 679, 79.
51. Uneyama, K., Kamaki, N., Moriya, A. and Torii, S. J. 1985, *Org. Chem.*, 50, 5396.
52. Vilanova, C., Sánchez-Péris, M., Roldán, S., Dhotare, B., Carda, M. and Chattopadhyay, A. 2013, *Tetrahedron Lett.*, 54, 6562.
53. Tanaka, H., Yamashita, S., Hamatani, T., Ikemoto, Y. and Torii, S. 1987, *Synth. Commun.*, 17, 789.
54. Wada, M., Ohki, H. and Akiba, K. -Y. 1990, *Bull. Chem. Soc. Jpn.*, 63, 1738.
55. Jadhav, B. D. and Pardeshi, S. K. 2014, *Tetrahedron Lett.*, 55, 4948.
56. Wada, M., Honna, M., Kuramoto, Y. and Miyoshi, N. 1997, *Bull. Chem. Soc. Jpn.*, 70, 2265.
57. Wada, M., Fukuma, T., Morioka, M., Takahashi, T. and Miyoshi, N. 1997, *Tetrahedron Lett.*, 38, 8045.
58. Ren, P. -D., Pan, S. -F., Dong, T. -W. and Wu, S. -H. 1996, *Chin. J. Chem.*, 14, 462.
59. Sawkmie, M. L., Paul, D., Khatua, S. and Chatterjee, P. N. 2019, *J. Chem. Sci.*, 131, 51.
60. Loh, T. -P., Tan, K. -T., Yang, J. -Y. and Xiang, C. -L. 2001, *Tetrahedron Lett.*, 42, 8701.
61. Gao, Y., Wang, X., Sun, L., Xue, L. and Xu, X. 2012, *Org. Biomol. Chem.*, 10, 3991.
62. Yoo, J., Oh, K. E., Keum, G., Kang, S. B. and Kim, Y. 2000, *Polyhedron*, 19, 549.
63. Zha, Z., Wang, Y., Yang, G., Zhang, L. and Wang, Z. 2002, *Green Chem.*, 4, 578.
64. Guimarães, R. L., Lima, D. J. P., Barros, M. E. S. B., Cavalcanti, L. N., Hallwass, F., Navarro, M., Bieber, L. W. and Malvestiti, I. 2007, *Molecules*, 12, 2089.
65. Wang, Z., Zha, Z. and Zhou, C. 2002, *Org. Lett.*, 4, 1683.
66. Zha, Z., Qiao, S., Jiang, J., Wang, Y., Miao, Q. and Wang, Z. 2005, *Tetrahedron*, 61, 2521.
67. Araki, S., Ito, H. and Batsugan, Y. J. 1988, *Organometallic Chem.*, 347, 5.
68. Sain, B., Prajapati, D. and Sandhu, S. J. 1992, *Tetrahedron Lett.*, 33, 4795.
69. Girard, P., Namy, J. L. and Kagan, H. B. 1980, *J. Am. Chem. Soc.*, 102, 2693.
70. Soupe, J., Namy, J. L. and Kagan, H. B. 1982, *Tetrahedron Lett.*, 23, 3497.
71. Basu, M. K. and Banik, B. K. 2001, *Tetrahedron Lett.*, 42, 187.
72. Jong, S. J. and Fang, J. M. 2001, *J. Org. Chem.*, 66, 3533.
73. Xu, X. and Zhang, Y. 2003, *Synth. Commun.*, 33, 3551.
74. Williams, D. R., Berliner, M. A., Stroup, B. W., Nag, P. P. and Clark, M. P. 2005, *Org. Lett.*, 7, 4099.
75. Wu, J. and Panek, J. S. 2010, *Angew. Chem. Int. Ed.*, 49, 6165.
76. Wu, J. and Panek, J. S. 2011, *J. Org. Chem.*, 76, 9900.
77. Matsuda, F., Sakai, T., Okada, N. and Miyashita, M. 1998, *Tetrahedron Lett.*, 39, 863.
78. Matsuda, F., Kito, M., Sakai, T., Okada, N., Miyashita, M. and Shirahama, H. 1999, *Tetrahedron*, 55, 14369.
79. Tamiya, H., Goto, K. and Matsuda, F. 2004, *Org. Lett.*, 6, 545.
80. Heumann, L. V. and Keck, G. E. 2007, *Org. Lett.*, 9, 1951.
81. Huang, J. and Yang, J. 2012, *Synlett*, 23, 737.
82. Huang, J., Yang, J. R., Zhang, J. and Yang, J. 2012, *J. Am. Chem. Soc.*, 134, 8806.

83. Huang, J., Yang, J. R., Zhang, J. and Yang, J. 2013, *Org. Biomol. Chem.*, 11, 3212.
84. Okude, Y., Hirano, S., Hiyama, T. and Nozaki, H. 1977, *J. Am. Chem. Soc.*, 99, 3179.
85. Jin, H., Uenishi, J., Christ, W. J. and Kishi, Y. 1986, *J. Am. Chem. Soc.*, 108, 5644.
86. Takai, K., Tagashira, M., Kuroda, T., Oshima, K., Utimoto, K. and Nozaki, H. 1986, *J. Am. Chem. Soc.*, 108, 6048.
87. Takai, K. and Nozaki, H. 2000, *Proc. Japan Acad.*, 76(B), 123.
88. Hargaden, G. C. and Guiry, P. J. 2007, *Adv. Synth. Catal.*, 349, 2407.
89. Hargaden, G. C. and Guiry, P. J. 2013, Stereoselective Nozaki-Hiyama-Kishi Reaction. In *Stereoselective Synthesis of Drugs and Natural Products*, Andrushko, V., Andrushko, N. (Eds), John Wiley & Sons, Ltd, 347.
90. Tian, Q. and Zhang, G. 2016, *Synthesis*, 48, 4038.
91. Gil, A., Albericio, F. and Álvarez, M. 2017, *Chem. Rev.*, 117, 8420.
92. Lachance, H. and Hall, D. G. 2008, *Org. React.*, 73, 1.
93. Lee, J. H. 2020, *Tetrahedron*, 76, 1.
94. Denmark, S. E. and Fu, J. 2003, *Chem. Rev.*, 103, 2763.
95. Kennedy, J. W. J. and Hall, D. G. 2003, *Angew. Chem. Int. Ed.*, 42, 4732.
96. Lambu, M. R., Hussain, A., Sharma, D. K., Yousuf, S. K., Singh, B., Tripathi, A. K. and Mukherjee, D. 2014, *RSC Adv.*, 4, 11023.
97. Lee, A. S. -Y., Chang, Y. -T., Wang, S. -H. and Chu, S. -F. 2002, *Tetrahedron Lett.*, 43, 8489.
98. Lim, J. W., Kim, K. H., Park, B. R. and Kim, J. N. 2011, *Tetrahedron Lett.*, 52, 6545.
99. Cho, Y. S., Lee, J. E., Pae, A. N., Choi, K. I. and Koh, H. Y. 1999, *Tetrahedron Lett.*, 40, 1725.
100. Masuyama, Y., Kishida, M. and Kurusu, Y. 1996, *Tetrahedron Lett.*, 37, 7103.
101. Masuyama, Y., Takeuchi, K. and Kurusu, Y. 2005, *Tetrahedron Lett.*, 46, 2861.
102. Jana, S., Guin, C. and Roy, S. C. 2004, *Tetrahedron Lett.*, 45, 6575.
103. Zhao, L. -M., Gao, H. -S., Li, D. -F., Dong, J., Sang, L. -L. and Ji, J. 2017, *Org. Biomol. Chem.*, 15, 4359.
104. Loh, T. -P., Zhou, J. -R. and Yin, Z. 1999, *Org. Lett.*, 1, 1855.
105. Hirayama, L. C., Gamsey, S., Kneuppel, D., Steiner, D., DeLaTorre, K. and Singaram, B. 2005, *Tetrahedron Lett.*, 46, 2315.
106. Nakamura, S., Hara, Y., Furukawa, T. and Hirashita, T. 2017, *RSC Adv.*, 7, 15582.
107. Appelt, H. R., Limberger, J. B., Weber, M., Rodrigues, O. E. D., Oliveira, J. S., Lüdtke, D. S. and Braga, A. L. 2008, *Tetrahedron Lett.*, 49, 4956.
108. Guo, R., Yang, Q., Tian, Q. and Zhang, G. 2017, *Sci. Rep.*, 7, 4873.
109. Steurer, S. and Podlech, J. 1999, *Eur. J. Org. Chem.*, 1991, 1551.
110. Reddy, D. S. and Corey, E. J. 2018, *J. Am. Chem. Soc.*, 140, 16909.
111. Lagoutte, R., Serba, C. and Winssinger, N. 2018, *J. Antibiot.*, 71, 248.
112. Hubert, J. G., Furkert, D. P. and Brimble, M. A. 2015, *J. Org. Chem.*, 80, 2231.
113. Zhao, Y. -M. and Maimone, T. J. 2015, *Angew. Chem. Int. Ed.*, 54, 1223.
114. Su, S., Rodriguez, R. A. and Baran, P. S. 2011, *J. Am. Chem. Soc.*, 133, 13922.
115. Bates, R. W. and Lek, T. G. 2014, *Synthesis*, 46, 1731.
116. Hu, X., Xu, S. and Maimone, T. J. 2017, *Angew. Chem. Int. Ed.*, 56, 1624.
117. Hu, X., Musacchio, A. J., Shen, X., Tao, Y. and Maimone, T. J. 2019, *J. Am. Chem. Soc.*, 141, 14904.
118. Yang, H., Gao, Y., Qiao, X., Xie, L. and Xu, X. 2011, *Org. Lett.*, 13, 3670.
119. Kumar, K. S. A., Rathee, J. S., Subramanian, M. and Chattopadhyay, S. J. 2013, *Org. Chem.*, 78, 7406.
120. Danishefsky, S. J., Deninno, M. P., Phillips, G. B., Zelle, R. E. and Lartey, P. A. 1986, *Tetrahedron*, 42, 2809.
121. Ma, X., Bolte, B., Banwell, M. G. and Willis, A. C. 2016, *Org. Lett.*, 18, 4226.
122. Bujaranipalli, S., Eppa, G. C. and Das, S. 2013, *Synlett*, 24, 1117.
123. Venkatesham, A. and Nagaiah, K. 2012, *Tetrahedron: Asymmetry*, 23, 1186.

-
124. Reddy, B. V. S., Reddy, B. P., Pandurangam, T. and Yadav, J. S. 2011, *Tetrahedron Lett.*, 52, 2306.
125. Kamal, A., Vangala, S. R., Reddy, N. V. S. and Reddy, V. S. 2009, *Tetrahedron: Asymmetry*, 20, 2589.
126. Alluraiah, G., Sreenivasulu, R., Murthy, I. S. and Raju, R. R. 2014, *Monatsh. Chem.*, 145, 2019.
127. Aher, R. D. and Sudalai, A. 2016, *Tetrahedron Lett.*, 57, 2021.
128. Marshall, J. A., Griot, C. A., Chobanian, H. R. and Myers, W. H. 2010, *Org. Lett.*, 12, 4328.
129. Zhang, W., Yao, H., Yu, J., Zhang, Z. and Tong, R. 2017, *Angew. Chem. Int. Ed.*, 56, 4787.